Research Square

Preprints are preliminary reports that have not undergone peer review.
They should not be considered conclusive, used to inform clinical practice,
or referenced by the media as validated information.

Behavioural States, Thermal Niche, Freshwater Habitat Selection, and Spatial Organisation of the Western Caspian Turtle, Mauremys Rivulata (Valenciennes 1833) (Testudines: Geoemydidae), in Southern Croatia

Maurivan Vaz Ribeiro
[2]EcoBrasil Consultoria Ambiental Ltda
Camila Brasil Louro Silveira
Institute of Geosciences, Federal University of Bahia
Katarina Koller Šarić
Association Hyla
Anja Neduk
Association Hyla
Ana Štih Koren
Association Hyla
Dragica Šalamon
dsalamon@agr.hr

Faculty of Agriculture, University of Zagreb, Croatia

Research Article

Keywords: movement ecology, hidden Markov model, individual repeatability, home range, Bhattacharyya overlap, thermal ecology

Posted Date: October 1st, 2026

DOI: https://doi.org/10.21203/rs.3.rs-11036103/v1

License: This work is licensed under a Creative Commons Attribution 4.0 International License.
Read Full License

Additional Declarations: No competing interests reported.

BEHAVIOURAL STATES, THERMAL NICHE, FRESHWATER HABITAT SELECTION, AND SPATIAL ORGANISATION OF THE WESTERN CASPIAN TURTLE, *MAUREMYS RIVULATA* (VALENCIENNES 1833) (TESTUDINES: GEOEMYDIDAE), IN SOUTHERN CROATIA

Maurivan Vaz Ribeiro[2,3], **Camila Brasil Louro da Silveira**[3], **Katarina Koller Šarić**[4], **Anja Neduk**[4], **Ana Štih Koren**[4], **Dragica Šalamon**[1]

[1]University of Zagreb, Faculty of Agriculture, Division of Animal Science, Svetošimunska 25, HR-10000 Zagreb, Croatia [Corresponding author: *D. Šalamon: dsalamon@agr.hr ,* https://orcid.org/0000-0003-3676-104X];

[2]EcoBrasil Consultoria Ambiental Ltda., Rua João Chagas Ortins de Freitas 577, Salvador, Bahia, CEP 42710-610, Brazil [*Ribeiro: maurivan.bio@gmail.com ,* https://orcid.org/0000-0003-3008-8640];

[3]Department of Oceanography, Institute of Geosciences, Federal University of Bahia – UFBA, Rua Barão de Jeremoabo s/n, Campus Universitário de Ondina, Salvador, Bahia, CEP 40170-290, Brazil [*Silveira: camilasilveira@ufba.br ,* https://orcid.org/0000-0001-9450-2164];

[4]Association Hyla, Lipovac I 7, Zagreb, Croatia [*Neduk: anja.neduk@hhdhyla.hr ,* https://orcid.org/0009-0000-6336-5048 *; Koller Šarić: katarina.koller@hhdhyla.hr ,* https://orcid.org/0000-0002-1997-5751 *; Štih Koren: ana.stih@hhdhyla.hr ,* https://orcid.org/0000-0003-3571-2457].

Behavioural states, thermal niche, freshwater habitat selection, and spatial organisation of the western Caspian turtle, *Mauremys rivulata* (Valenciennes 1833) (Testudines: Geoemydidae), in southern Croatia

ABSTRACT. — We present a behaviourally resolved telemetric baseline for the western Caspian turtle, *Mauremys rivulata* (Valenciennes 1833), at the north-western edge of its range, in southern Croatia. Sixteen adults were tracked with GNSS-temperature loggers (April 2025–June 2026); 15 returned 3,327 fixes retained after coordinate validity checks, per-individual density-based spatial clustering of applications with noise (DBSCAN) main-cluster filtering, and speed filtering (nine females, six males). A hidden Markov model identified two persistent behavioural states, Slow (42.5%) and Fast (57.5%), with Fast fixes occurring at warmer transmitter temperatures (+4.7 °C). Activity was strongly seasonal: the Fast state peaked during the nesting period (June–July, 70.9%) and collapsed at the August thermal peak (25.1%), consistent with a thermal-refuge response at the population level. Signal blocking from late October to late February indicates brumation period. Five of seven behavioural traits were weakly repeatable (R = 0.10–0.27). Individual median speed and Fast-state use were positively correlated (Spearman $\rho = 0.79$, $p = 0.036$), indicating a weak fast-movement axis. Home ranges, estimated by autocorrelation-corrected kernel density, spanned three orders of magnitude (0.09–103.1 ha; median 4.4 ha) and were unrelated to sex. Pairwise spatial overlap was low across all dyads, and an integrated step-selection function showed strong selection for proximity to surface water in both Fast and Slow states. Movement up to 30 m away from the aquatic part of the habitat spiked in May. Together, these results depict a thermally regulated, water-dependent species organised into discrete, high-fidelity perennial freshwater habitat units, with each pond cluster, intermittent river, ephemeral stream, or canal functioning as independent spatial conservation unit.

KEYWORDS. — movement ecology; hidden Markov model; individual repeatability; home range; Bhattacharyya overlap; thermal ecology

BACKGROUND

Movement is the trait through which animals reconcile competing physiological, ecological, and reproductive demands, and the resulting trajectories carry the signatures of every selective pressure that shapes this reconciliation (Nathan et al. 2008; Kays et al. 2015). For ectothermic vertebrates, movement is additionally constrained by the thermal environment, because locomotor capacity, digestion, and reproductive output depend on body temperature (Huey and Stevenson 1979; Angilletta 2009), and individuals shuttle between thermally distinct microhabitats to keep operative temperatures within performance-relevant ranges (Hertz et al. 1993). Freshwater turtles combine prolonged inactivity with brief bouts of directed movement across aquatic, thermoregulatory, and terrestrial microhabitats, making them an instructive system for investigating how behavioural architecture, thermal niche, and landscape structure jointly shape space use (Bury 1979; Lebboroni and Chelazzi 1991; Rowe and Dalgarn 2010).

Hidden Markov models (HMMs) decompose a continuous trajectory into a small number of discrete states whose emission distributions carry biologically intuitive labels and whose persistence on the diagonal of the transition matrix encodes the temporal grain of behavioural switching (Patterson et al. 2009; Langrock et al. 2012; McClintock and Michelot 2018). Repeatability analysis partitions behavioural variance into among- and within-individual components, providing a formal test of the behavioural consistency that underpins the animal personality literature (Sih et al. 2004; Réale et al. 2007; Stoffel et al. 2017; Dammhahn et al. 2018). Used together with home-range and spatial-overlap estimation, these methods produce a multiscale portrait in which the HMM identifies what an individual is doing at each fix, the integrated step-selection function (iSSF) identifies the landscape features it selects when moving, and repeatability quantifies how much of the among-fix variance is locked into stable individual differences. For a stream-dwelling chelonian whose food and thermal resources are concentrated along a narrow water-margin ribbon, the central empirical question is how strongly hydrography itself constrains habitat selection, and whether sex, individual identity, and season carve detectable structure on top of that constraint (Klappstein et al. 2023).

The western Caspian turtle, *Mauremys rivulata* (Valenciennes, 1833), is a Mediterranean freshwater terrapin distributed from the southern Balkans, across Anatolia, to the Levant, with disjunct insular populations (Vamberger et al. 2014; Thomson 2021). It is classified as Least Concern globally, but Near Threatened in several national assessments, with an unfavourable conservation status for populations and habitats in Europe based on national Habitat Directive reporting, due to agricultural land-use change, water management and loss of water bodies, and the spread of the invasive *Trachemys scripta* (Cordero-Rivera and Ayres 2004; Popgeorgiev 2017). Three extant *M. rivulata* populations in Croatia are northern and western range-edge populations inhabiting the extreme south of the country: Konavle polje (karst polje/field; Seware, 2024), the Majkovi area (ponds in the hamlets of Zabrežje and Prljevići) and Ston polje at the north-western edge of the species' range, within the Natura 2000 network (Figure 1). Two self-sustaining extant Croatian populations were the focus of this research: the Konavle population, the largest and demographically stable (about 350 adults), and the Majkovi population, comprising Zabrežje and Prljevići, smaller but stable (about 130 adults) (Štih Koren 2024). The Ston population (south-eastern Pelješac Natura 2000 site: HR2001364) is not self-sustaining and is being supplemented with 100 juveniles through a conservation-breeding programme 2026 - 2031. A former Ombla River population (the Significant Landscape of Rijeka Dubrovačka) is assessed as non-viable within an urbanised environment (MINGOR 2021). At these sites, animals occupy a network of artificial and secondary ponds, seasonal karst streams (intermittent rivers and ephemeral streams), and ephemeral and perennial amelioration canals embedded in an agriculturally cultivated matrix (Crnobrnja-Isailović et al. 2018; Štih Koren 2024). Despite the inclusion of the species in regional herpetological surveys, no quantitative, telemetry-based behavioural baseline has been published for the Croatian population, and telemetry-derived knowledge remains limited for *M. rivulata,* with only a few studies available (e.g. Chelazzi et al. 2007; Levi et al. 2025).

The aims of the study were to: (i) identify the discrete behavioural states that best describe movement trajectories of the adult *M. rivulata* population and estimate their temporal persistence; (ii) characterise the thermal niche associated with the adult behavioural states and with individual sex with sex treated as an

exploratory, rather than confirmatory factor; (iii) estimate among-individual repeatability of seven behavioural traits and assess whether the repeatable traits form a consistent fast-movement axis; (iv) estimate adult individual home ranges using three methods, adopting autocorrelational kernel density estimation (AKDE) as the primary estimator when continuous-time movement model selection confirmed range residency; (v) quantify pairwise spatial overlap with the Bhattacharyya coefficient, compare the three home-range estimators, and test home-range overlap; (vi) assess seasonal variation in adult thermal niche and behavioural-state proportions by dividing the active season into four functional periods; and (vii) quantify fine-scale habitat selection of adult *M. rivulata* with an integrated step-selection function (iSSF), testing whether individuals select steps that keep them close to the hydrographic network. Throughout, the study emphasises microhabitat use and seasonal life-history structure.

METHODS

We structured our procedures for animal sample capture, data collection and reporting of results in accordance with the STRANGE framework (Webster and Rutz 2020) to ensure transparency and address potential sampling biases related to capture vulnerability, animal health, and sex ratio. Potential influences on sample representativeness (e.g. trap happiness, body condition thresholds and sex-specific spatial sampling limitations), as well as the sampling plan and its success, are explicitly accounted for in our choice of analyses and discussed.

Sampling: study area, capture, and instrumentation

Transmitter data collection was conducted from April 2025 to June 2026 in the Konavle polje (42.52–42.57°N, 18.30–18.38°E) and the Majkovi area (42.77°N, 17.91°E), southern Croatia (Figure 1). The Konavle polje is a karst lowland with a dense network of artificial and secondary ponds, the perennial Konavočica and Kopačica Rivers, and perennial, ephemeral, and intermittent karst streams, and amelioration canals. The Majkovi area comprises three small secondary ponds and ephemeral karst streams set within a Mediterranean hill-karst landscape. Both sampling areas lie within the Natura 2000 network:

123 “Sniježnica and Konavle polje” (site HR2000946), and the Majkovi area (“Zabrežje” and “Prljevići”: sites
124 HR2000947 and HR2000555).

125 The animal capture design aimed to achieve: (i) a 1:1 sex ratio corresponding to the observed population
126 ratio across the two populations; (ii) a 1:3 ratio of individuals captured from the Majkovi and Konavle
127 populations to reflect their relative population sizes; (iii) capture localities that included distinct aquatic
128 microhabitats while minimizing localised selection bias. These localities comprised secondary ponds in
129 forest and open agricultural mosaic, the intermittent Konavočica river, perennial and ephemeral streams
130 and canals situated on the slopes of Mount Sniježnica, and in the Konavle polje lowland, as well as all three
131 secondary ponds in Majkovi.

132 Sixteen adult *M. rivulata* captured during April 2025 with baited funnel traps were instrumented (nine
133 females, seven males). Animals were measured for straight carapace length and body mass (Supplementary
134 Table S1) to ensure recommended ≤ 5% device mass relative to the body mass of the smallest instrumented
135 adult, sexed by tail morphology and plastral concavity, individually marked and equipped with lightweight
136 (8.4 g, 43 mm x 25 mm x 12 mm) GNSS-temperature data loggers (Interrex Series, Druid Technology Co.,
137 Ltd., Chengdu, China). Loggers were attached to the carapace between pleural scutes 1 and 2 using fast-
138 curing acrylic resin with accelerator (Technovit® 6091, Kulzer GmbH, Wehrheim, Germany), applied in
139 several thin layers in a rectangular shape matching the transmitter, reducing the application surface.
140 Animals were monitored on site for 6 hours to confirm that each animal retained control of swimming and
141 diving, and were released at the capture location.

142 Solar- battery loggers were programmed for repeated GNSS (global navigation satellite system) fix attempts
143 at a target sub-hourly to hourly cadence during the day, with temperature recorded hourly. Realised median
144 fix intervals varied widely among individuals (from about 0.5 h to several hours; Table 1). Data
145 transmission was programmed via 4G/5G network utilising narrow-band cellular connectivity (NB-IoT)
146 and scheduled every 48 hours, with a contingency plan of periodic manual connection via Bluetooth.

147

Table 1. Summary of tracking data per individual *Mauremys rivulata* from two populations in Croatia.

Code	Sex	Locality	GNSS fixes	Temp. obs.	Duration (d)	Median Δt (h)	Tracking period
81F	F	Konavočica River (Gruda)	224	183	399	2.99	04 May 2025 – 07 Jun 2026
822	F	Konavle pond (playground)	190	0	76	1.33	29 Apr – 14 Jul 2025
81C	F	Konavle pond 5	188	188	154	4.16	29 Apr – 30 Sep 2025
816	F	Konavle pond 14	172	171	400	3.34	01 May 2025 – 05 Jun 2026
819	F	Konavle pond 1	165	1	346	2.47	30 Apr 2025 – 11 Apr 2026
823	F	Zabrezje crkva	39	1	161	29.01	30 Apr – 08 Oct 2025
820	F	Zabrezje DVD	25	11	363	12.79	27 Apr 2025 – 25 Apr 2026
80C	F	Pridvorje monastery pond	21	20	121	104.87	17 May – 15 Sep 2025
81E	F	Konavle pond 17	8	8	360	218.31	05 Jun 2025 – 31 May 2026
821	M	Konavle pond 4	1,587	443	404	0.49	29 Apr 2025 – 07 Jun 2026
824	M	Konavle canal 16	670	101	391	0.83	29 Apr 2025 – 25 May 2026
814	M	Konavle pond 10b	24	24	40	23.02	08 May – 17 Jun 2025
825	M	Konavočica River (Gruda)	7	7	126	517.63	09 Jun – 13 Oct 2025
80F	M	Majkovi church	4	4	0.1	0.34	01 May 2025
81B	M	Konavočica River (Gruda)	3	3	16	192.27	22 May – 07 Jun 2025

Individuals 80F, 81B, 81E, and 825 are excluded from the individual home-range (AKDE), repeatability, and overlap analyses owing to insufficient tracking duration or number of fixes. Temp. obs.: counts the paired transmitter-temperature observations; M: male; F: female.

All research procedures were planned to comply with ethical treatment guidelines (ASAB Ethical Committee/ABS Animal Care Committee, 2023) and were ethically reviewed and approved by the Bioethical Committee for Animal Protection and Welfare of the University of Zagreb Faculty of Agriculture. Procedures involving this protected species comply with Croatian animal welfare, research

and nature protection legislation, under permits issued by the Croatian Ministry of Economy and Sustainable Development (Permits No. UP/I-352-04/25-08/147 and UP/I-352-04/23-08/148).

Trajectory cleaning and standardisation

Raw transmitter records were filtered in three steps: (1) removal of records without valid coordinates; (2) a main-cluster density-based spatial clustering of applications with noise (DBSCAN) filter, applied per individual in projected Universal Transverse Mercator (UTM) coordinates (eps = 5 km, minPts = 3) to discard isolated points; and (3) application of a biologically plausible speed threshold of 0.40 m s^{-1} (Lebboroni and Chelazzi 1991). After filtering, the dataset contained 3,327 valid GNSS fixes from 15 individuals (Table 1). To minimise observer bias in the analysis, blinded methods were used, including random IDs, obscured sex information where this information was not necessary, and randomised order of the time series.

All coordinates were projected to EPSG:32633 (UTM zone 33N) for metric computation, and step length, time interval, and step speed were recomputed from the projected coordinates and checked against the archived values (Pearson $r > 0.9999$). Individuals were retained for the individual-level spatial analyses (AKDE, overlap, repeatability) only when they met an a priori spatial-adequacy threshold of ≥ 12 GNSS fixes and ≥ 14 days of tracking. Because the main-cluster filter was applied per individual, a few transmitters retained in earlier drafts fell below this threshold after the stricter cleaning.

Behavioural states (Gaussian hidden Markov model, HMM)

Behavioural states were decoded with a Gaussian hidden Markov model (HMM) on the standardised logarithm of step speed, an approach consistent with the use of HMMs to infer latent movement states from time series of animal displacement (Morales et al. 2004; Langrock et al. 2012; Patterson et al. 2017; McClintock et al. 2020). The analysis was restricted to consecutive observations with $\Delta t < 12$ h, to reduce step-length distortion caused by highly heterogeneous observation intervals, a recognised limitation of discrete step-based movement models that depend on the temporal resolution of the data (Langrock et al. 2012; Patterson et al. 2017; Michelot and Storey 2025).

Models with k = 2, 3, and 4 states were fitted, each with 30 random initialisations, retaining the best model per k. This procedure is recommended because maximum-likelihood estimation in HMMs can be sensitive to local maxima and to initial parameter values (Zucchini et al. 2016; Glennie et al. 2023). The number of states was assessed using the Bayesian information criterion (BIC), widely employed to compare HMMs of differing complexity, together with complementary diagnostics of stability and ecological plausibility (Zucchini et al. 2016; McClintock et al. 2020; Glennie et al. 2023).

States were labelled by emission speed as Slow and Fast, rather than as validated behaviours, because HMMs fitted only to kinematic variables infer latent movement modes that may serve as behavioural proxies but do not constitute direct behavioural validation without independent evidence such as direct observation, additional sensors, or external behavioural covariates (Patterson et al. 2008; Michelot et al. 2016; McClintock and Michelot 2018; Glennie et al. 2023).

Thermal niche

Transmitter temperature is an integrated indicator of microhabitat and of the animal's metabolic heat, and not a direct measure of core body temperature. Transmitter temperature was paired with HMM state and individual sex. Differences between states and between sexes were tested by Kruskal–Wallis rank test and by Mann–Whitney U test (two-tailed), respectively, and monthly cycles were summarised as median ± standard deviation (SD) per month.

Behavioural repeatability and syndrome structure

Behavioural traits were aggregated into ISO weeks with ≥ 5 fixes per individual, totalling 135 sessions from 7 individuals after excluding those with < 3 sessions. We tested seven behavioural traits: median and mean step speed, coefficient of variation of speed, log maximum displacement, logit proportions of the Fast and Slow states, and mean transmitter temperature. Repeatability (R) was estimated as the intraclass correlation coefficient (ICC1) by one-way variance decomposition (Stoffel et al. 2017). The 95% confidence intervals (CI) were obtained by individual-clustered bootstrap (500 resamples), and significance by permutation of individual labels (999 permutations), with p adjusted by the Benjamini–Hochberg false discovery rate

(FDR) (Benjamini and Hochberg 1995). Among-individual covariation was assessed by Spearman correlation between individual means.

Home range and pairwise overlap

Home ranges were estimated using three complementary methods. Minimum convex polygons (MCP) 50% and 95%, and kernel density estimation (KDE) 50% and 95% with per-individual Silverman bandwidth, were used as conventional estimators, allowing comparison with previous studies based on traditional home-range methods (Silverman 1986; Worton 1989; Seaman et al. 1999; Börger et al. 2006). As the primary estimator, we adopted autocorrelated kernel density estimation (AKDE), which explicitly incorporates temporal autocorrelation of trajectories and reduces the bias associated with assuming independence between successive fixes, especially in telemetry data with irregular or autocorrelated sampling (Fleming et al. 2015; Fleming and Calabrese 2017; Silva et al. 2022). For each individual, we fitted continuous-time movement models (independent and identically distributed: IID; Ornstein-Uhlenbeck: OU; and Ornstein-Uhlenbeck Foraging / Velocity-Correlated: OUf; isotropic and anisotropic) and selected the best by Akaike Information Criterion with Correction for Small Sample Sizes (AICc), following the approach implemented in the continuous-time movement modelling (ctmm) framework for home-range estimation from continuous-time stochastic processes (Calabrese et al. 2016; Fleming and Calabrese 2017). Empirical variograms were used to check saturation and visually validate the selected fit (Fig. 5), a recommended step for assessing spatial residency, autocorrelation structure, and movement-model adequacy before AKDE home-range estimation (Calabrese et al. 2016; Silva et al. 2022).

Model selection acts as a formal filter of sampling adequacy, because telemetry-based home-range estimates are sensitive to the number of fixes, temporal autocorrelation, sampling resolution, and the spatial representativeness of trajectories (Seaman et al. 1999; Börger et al. 2006; Fleming et al. 2015; Silva et al. 2022). Individuals with fewer than five fixes do not support model fitting and were excluded from AKDE estimation, because this estimator depends on the selection of an informative movement model and on data sufficient to characterise the temporal structure of individual displacement (Fleming et al. 2015; Calabrese

et al. 2016; Silva et al. 2022). The three estimators were compared pairwise using individual-paired Wilcoxon tests (MCP vs KDE, KDE vs AKDE, and MCP vs AKDE, at 50% and 95%), and sex effects on each estimator were tested with two-tailed Mann–Whitney U tests, both appropriate when comparisons involve small samples and normality cannot be assumed (Wilcoxon 1945; Mann and Whitney 1947; Hollander et al. 2014). The relationship between home-range size and number of fixes was assessed with Pearson correlation to check for estimator bias from sampling effort, a recurrent concern in conventional and autocorrelated home-range estimates (Seaman et al. 1999; Börger et al. 2006; Fleming et al. 2015; Silva et al. 2022).

Pairwise overlap was quantified with the Bhattacharyya coefficient (BC) via numerical integration on a common grid with per-individual bandwidths, restricted to the 11 individuals with adequate spatial sampling (≥ 12 fixes and ≥ 14 d of tracking). This restriction reduces the influence of insufficiently sampled trajectories and circumvents the sensitivity of overlap estimates to pooled-bandwidth choices, a recognised problem in analyses based on utilisation distributions (Fieberg and Kochanny 2005; Winner et al. 2018). The BC was adopted because it quantifies similarity between utilisation distributions and is more informative than the simple geometric intersection of home-range polygons when the goal is to assess the relative intensity of shared space use (Fieberg and Kochanny 2005). Contrasts of mean BC among dyad types were assessed by an individual-level permutation test, with 1,000 random sex assignments, an approach appropriate for avoiding pseudoreplication when multiple dyads share the same individuals (Manly 2007; Winner et al. 2018).

Habitat-selection analysis: integrated step-selection function (iSSF).

Fine-scale habitat selection was assessed using an integrated step-selection function (iSSF) fitted with conditional logistic regression, an approach that compares used steps with paired available steps within the same stratum and allows resource- selection and movement-process components to be estimated simultaneously (Fortin et al. 2005; Thurfjell et al. 2014; Avgar et al. 2016). We retained 2,506 used steps from eight individuals with regular consecutive fixes, because SSF/iSSF inference depends on a coherent

definition of steps between successive fixes and a sufficiently consistent temporal scale among observations (Forester et al. 2009; Thurfjell et al. 2014; Avgar et al. 2016). For each used step, 50 available steps were generated by resampling the observed step lengths and turn angles, totalling 125,300 available steps, a procedure consistent with the construction of case–control sets in SSF/iSSF and with recommendations to sample available movements from the observed empirical movement distribution (Fortin et al. 2005; Forester et al. 2009; Thurfjell et al. 2014; Avgar et al. 2016).

The habitat covariate was the log Euclidean distance to the union of the official Croatian hydrography layers, a continuous proximity metric suitable for assessing selection across environmental gradients when the expected ecological response is associated with distance to linear features or habitat patches (Boyce et al. 2002; Manly et al. 2002; Fortin et al. 2005). The consistency of this covariate was verified by subsampling (Pearson r = 0.99). Log step length and the cosine of the turn angle were also included, movement terms commonly incorporated in iSSF to control for the locomotor process and to separate, as far as possible, habitat selection from movement-induced availability (Forester et al. 2009; Avgar et al. 2016; Signer et al. 2019).

Covariates were z-standardised, allowing the coefficients to be expressed as relative selection strengths (RSS = exp(β)) per standard deviation. This interpretation is compatible with resource-selection models estimated on a relative scale, in which exponentiated coefficient ratios represent proportional changes in relative selection associated with covariate variation (Manly et al. 2002; Lele et al. 2013; Avgar et al. 2017). The model was stratified by step, and coefficient significance was assessed using Wald tests, a usual procedure in conditional logistic regression applied to paired step-selection designs (Fortin et al. 2005; Thurfjell et al. 2014; Avgar et al. 2016).

Seasonal classification

Fixes were grouped into four functional periods of the active season: putative mating (April–May), putative nesting (June–July), thermal peak (August), and prebrumation (September–October). No fixes from instruments that resumed transmission after December 2025 are considered as device signal blocking is

attributed to overwintering behaviour and microhabitat. The April–May label follows the timing of the reproductive (testicular) cycle reported for the species by Gasith and Sidis (1985). We did not observe mating directly, so this period is defined a priori from the literature rather than inferred from the present movement data. Among these periods, we compared transmitter temperature, HMM state proportions, and median step speed using Kruskal–Wallis and chi-square tests (two-tailed $\alpha = 0.05$).

Statistical framework and reproducibility

Analyses were conducted in Python 3.12 using the libraries NumPy, pandas, SciPy, statsmodels, hmmlearn, scikit-learn, and matplotlib. Continuous-time movement and AKDE estimation followed the ctmm framework (Fleming et al. 2015; Calabrese et al. 2016) in RStudio (R Core Team 2026). Statistical significance was set at $\alpha = 0.05$; within-family multiple comparisons (seven repeatability traits) were adjusted by FDR (Benjamini and Hochberg 1995).

RESULTS

Sample and sampling effort

Of the 16 deployed transmitters, 15 generated valid GNSS data; individual 817 recorded temperature only. After applying the speed and DBSCAN clustering filters, 3,327 fixes were retained from the 15 GNSS-active individuals (nine females, six males; Table 1). Data sampling result was highly uneven: male 821, from Konavle pond 4, was the most-tracked individual, with 1,587 fixes over 404 days, whereas fixes from four individuals 81E (eight fixes), 825 (seven fixes), 80F (four fixes), and 81B (three fixes) fell below the analytical minimum for reliable home-range estimates (Figure 2).

Overlap analyses included 11 individuals with adequate spatial sampling (eight females, three males). Autocorrelational kernel density estimation (AKDE) estimates were restricted to the nine individuals that selected range-residency models (six females, three males), and seven individuals contributed to the repeatability analyses (Table 1). This unevenness by sex and location reflects technical issues in data return: the realised number of fixes was strongly conditioned by Global System for Mobile Communications

(GSM) reception, which is poor in the Majkovi area and yielded few fixes for several Zabrežje individuals (e.g. 823, 39 fixes; 820, 25 fixes) and none for Prljevići individuals (817, zero fixes). By sex, the cleaned dataset comprised 1,032 fixes for females and 2,295 for males; the male total is dominated by individual 821, which alone contributed 1,587 fixes (69% of all male fixes and 48% of the whole dataset). Sex differences are reported where detected but are explicitly qualified because adequate spatial sampling was achieved for far fewer males than females. Nevertheless, the structure of the collected data enabled testing of the thermal niche by sex. Per-individual cleaned tracks are available in the Zenodo open dataset.

Body size and mass

Biometric data measured at capture (April 2025) were available for the instrumented adults: straight carapace length (SCL) for 10 individuals and body mass for 12 (Supplementary Table S1). Mean SCL was 153.1 ± 28.5 mm (range 104.2–187.8 mm) and did not differ between sexes (females 152.4 ± 33.3 mm, n = 6; males 154.1 ± 24.3 mm, n = 4; Mann–Whitney U = 13.0, p = 0.914). Mean body mass was 581 ± 129 g (range 363–761 g); females tended to be heavier than males (females 633 ± 99 g, n = 7; males 508 ± 140 g, n = 5), but the difference was not significant (Mann–Whitney U = 28.5, p = 0.087). The lightest instrumented adult weighed 363 g (male 821), so the loggers (weighing 8.4 g) represented ≤ 2.5% of body mass for every animal, as required for attachment (implied logger mass ≤ ~18 g). The carapace-length–mass relationship was heterogeneous: the three previously captive-held Majkovi animals (80F, 823, 820) were comparatively short but heavy, so this group should be verified against the field sheets before any allometric interpretation.

Behavioural states

Although the three-state model had the lowest BIC (6,715.8; Table 2) and met the biological filters, its stability was low: the optimum appeared in only 13 of 60 initialisations, compared with 37 for the two-state model. Moreover, the within-individual autocorrelation in log step speed ($r \approx 0.20$; variance inflation ≈ 1.5) reduces the effective sample size and probably overestimates the nominal support for the third state (ΔBIC

= 8.4). We therefore retained the two-state model, which was more reproducible and well separated (Figure 2A–C).

Table 2. HMM model-selection diagnostics for behavioural states of *Mauremys rivulata*.

k	Log-likelihood	BIC	AIC	Parameters	Min. speed ratio	Min. P(diag)	Init. at optimum (/60)
2	−3,334.8	6,724.2	6,683.5	7	4.56	0.86	37
3	−3,303.2	6,715.8	6,634.5	14	2.14	0.84	13
4	−3,282.3	6,744.1	6,610.6	23	1.20	0.61	—

Selection by BIC together with a reproducibility check (fraction of 60 initialisations recovering the global optimum) and biological-plausibility filters.

The states were interpreted as Slow and Fast. The Slow state included 1,045 fixes (42.5%), with a median speed of 0.0021 m s^{-1} and a median step of 7.6 m; the Fast state included 1,412 fixes (57.5%), with a median speed of 0.0103 m s^{-1} and a median step of 9.4 m (Table 3). Both showed high persistence (P(S→S) = 0.86; P(F→F) = 0.89; Figure 2C).

Table 3. Characteristics of the HMM states for k = 2 (2,457 decoded fixes from 14 individuals).

State	Fixes	%	Median speed (m/s)	Mean speed (m/s)	Median step (m)	Temperature observations	Median T (°C)
Slow	1,045	42.5	0.0021	0.0035	7.6	313	35.0
Fast	1,412	57.5	0.0103	0.0176	9.4	437	39.7

Thermal niche

Transmitter temperature was recorded at 1,165 of the 3,327 cleaned fixes (35.0%) over the campaign. The thermal niche varied with behavioural state: Fast fixes had a median of 39.7 °C (n = 437), whereas Slow fixes recorded 35.0 °C (n = 313), a difference of 4.7 °C (Kruskal–Wallis H = 85.8, df = 1, $p < 0.001$; Figure 2D). There was also a statistical difference between sexes, but of small magnitude: females (n = 583) had a median of 37.9 °C and males (n = 582) 37.2 °C, a difference of 0.7 °C (Mann–Whitney U = 189,331, p =

0.001; Figure 2E). The seasonal profile was unimodal: median temperature rose from about 21–35 °C in the early transitional season to a peak of 41.2 °C in August, then fell to roughly 27–29 °C in late autumn (Figure 2F).

Seasonal patterns

The four functional periods with transmission were well represented in the sample (Table 10). Transmitter temperature varied significantly among periods (Kruskal–Wallis $H = 59.3$, $p < 0.001$): the median rose from 37.2 °C in the putative mating period to 40.0 °C in the putative nesting period, reached 41.2 °C at the August thermal peak, and then fell to 34.6 °C in prebrumation (Fig. 4A). Hidden Markov model (HMM) state proportions also changed markedly across the season ($\chi^2 = 212.8$, $df = 3$, $p < 0.001$). The proportion of the Fast state was maximal in the putative nesting period (70.9%), fell to 25.1% in August, and then increased partially in prebrumation (35.1%; Fig. 4B). Median step speed followed the same pattern, with the highest value in the putative nesting period (0.0044 m s^{-1}) and the lowest at the August thermal peak (0.0014 m s^{-1}; Kruskal–Wallis $H = 103.5$, $p < 0.001$; Fig. 4C).

Table 10. Seasonal stratification of *Mauremys rivulata* movement data by functional period.

Functional period (months)	Fixes	Fast prop. (%)	Median speed (m/s)	Temp. obs.	Median T (°C)
Putative mating (Apr–May)	1,231	56.9	0.00329	644	37.2
Putative nesting (Jun–Jul)	1,281	70.9	0.00438	207	40.0
Thermal peak (Aug)	287	25.1	0.00138	59	41.2
Prebrumation (Sep–Oct)	432	35.1	0.00163	163	34.6
Overwintering (Nov–Mar)	96	—	—	92	33.5

Fast prop.: Fast-state proportion from HMM-decoded fixes; median step speed and temperature are descriptive medians per period.

Additionally, dry-land fixes (30 m from water body) by females and males were observed to be starting from May. These fixes—inside versus outside water, resolved by month and sex—are summarised as

complementary illustrative material (Supplementary Figure S2). Females made dry-land movements throughout the active season, peaking during the putative nesting window, whereas males were almost exclusively aquatic apart from a small spring signal. The classification presented in Supplementary Figure S2 is robust to the distance threshold; distances of 20, 30, and 50 m give near-identical results.

Movement effectively ceased after late October. Outside the four active-season periods, only 96 fixes were recorded during the winter window (November to March) following the transmission gap from late October to late February (Table 10). These fixes correspond to four animals (two females and two males) transmitting in late February (one individual) and early March (in Konavle: 816 and 821 in ponds, 824 in canals and ponds, and 819 in canals) with a median recorded temperature of 33.5 °C (range 10.4–45.4 °C). Long-distance winter movement was recorded in only one individual, which travelled 800 m to the southern part of the Konavle polje. In 2026 putative mating period, seven individuals (816, 819, 81E, 81F, 820, 821, 824) produced renewed fixes.

Behavioural traits repeatability and among-individual covariation

Five of the seven behavioural traits were repeatable after false discovery rate correction, always with modest magnitudes (Table 4; Fig. 3A). The highest repeatability occurred for mean transmitter temperature (R = 0.27, 95% CI [0.00, 0.35], p_adj = 0.004), followed by median step speed (R = 0.17, p_adj = 0.004), log maximum displacement (R = 0.12, p_adj = 0.012), and the Fast- and Slow-state proportions (R = 0.10, p_adj = 0.014). Mean step speed (R = 0.02) and the coefficient of variation of speed (R = 0.01) were not repeatable. Individual median speed was positively correlated with the mean proportion of the Fast state (ρ = 0.79, n = 7, p = 0.036).

Table 4. Among-individual repeatability of *Mauremys rivulata* behavioural traits.

Trait	Observations	Individuals	R	95% CI	p_adj	Signif.
Median step speed (m/s)	135	7	0.17	[0.00, 0.22]	0.004	*
Mean step speed (m/s)	135	7	0.02	[0.00, 0.13]	0.272	
Coefficient of variation: speed	135	7	0.01	[0.00, 0.04]	0.327	

Trait	Observations	Individuals	R	95% CI	p_adj	Signif.
Log maximum displacement (m)	135	7	0.12	[0.00, 0.27]	0.012	*
Fast-state proportion (logit)	135	7	0.10	[0.00, 0.18]	0.014	*
Slow-state proportion (logit)	135	7	0.10	[0.00, 0.18]	0.014	*
Mean transmitter temperature (°C)	65	5	0.27	[0.00, 0.35]	0.004	*

R: ICC1 from a one-way variance-component decomposition; 95% CI: obtained by clustered bootstrap (500 resamples); p: significance obtained by permutation test (999 permutations); p_adj: the Benjamini–Hochberg false discovery rate; *: p_adj < 0.05.

Home range

Table 6. *Mauremys rivulata* home-range estimates: minimum convex polygon (MCP) and kernel density (KDE).

Code	Sex	Locality	Fixes	MCP 50%	MCP 95%	KDE 50%	KDE 95%
819	F	Konavle pond 1	165	1.680	17.851	7.454	36.959
81B *	M	Konavočica River (Gruda)	3	1.951	1.951	7.197	25.177
80C	F	Pridvorje monastery pond	21	0.219	4.770	3.852	18.118
81E *	F	Konavle pond 17	8	1.380	2.030	2.642	11.108
816	F	Konavle pond 14	172	3.550	9.769	2.239	10.710
821	M	Konavle pond 4	1,587	3.407	5.859	1.149	5.541
81F	F	Konavočica River (Gruda)	224	0.678	5.067	0.734	3.977
825 *	M	Konavočica River (Gruda)	7	0.007	0.030	0.502	2.202
81C	F	Konavle pond 5	188	0.911	1.473	0.436	2.198
824	M	Konavle canal 16	670	0.467	2.009	0.274	2.038
823	F	Zabrezje church	39	0.048	0.616	0.152	1.024
822	F	Konavle pond (playground)	190	0.059	0.615	0.080	0.542
820	F	Zabrezje DVD	25	0.006	0.033	0.024	0.127

Code	Sex	Locality	Fixes	MCP 50%	MCP 95%	KDE 50%	KDE 95%
814	M	Konavle pond 10b	24	0.008	0.027	0.025	0.101
80F *	M	Majkovi church	4	0.005	0.001	0.013	0.048

Home- range estimates are given for the 15 GNSS-active individuals, ordered by decreasing KDE 95%. Areas in hectares, computed in UTM 33N; KDE bandwidth per individual by Silverman's rule. * indicates an individual with sampling below the spatial-adequacy threshold (≥ 12 fixes and ≥ 14 d), excluded from AKDE and overlap analyses.

Continuous-time movement models indicated autocorrelated range residency (Ornstein-Uhlenbeck family, OU) in nine individuals: six females (816, 819, 81C, 81F, 822, 823) and three males (814, 821, 824). Four individuals selected IID models (independent and identically distributed), in which AKDE equals KDE, and two had fewer than five fixes, preventing the fit. The variograms and ctmm models (Fig. 5) support this classification, with clear plateaus in well-sampled individuals and low information in sparse trajectories. Home range estimates by minimum convex polygon (MCP) and kernel density (KDE) for the 15 GNSS-active individuals are given in Table 6, Figure 6, and Figure 7. Home-range estimates by autocorrelation-corrected kernel density (AKDE) for the nine individuals that selected continuous-time range-residency movement models are given in Table 7 and Figure 8.

Table 7. *Mauremys rivulata* home-range estimates by autocorrelation-corrected kernel density (AKDE).

Code	Sex	Fixes	Selected model	AKDE 95% (95% CI)	AKDE 50% (95% CI)
819	F	165	OU anisotropic	103.14 (58.87–159.63)	26.67 (15.22–41.27)
816	F	172	OU anisotropic	33.36 (18.32–52.83)	8.74 (4.80–13.84)
81F	F	224	OU	21.96 (13.67–32.19)	4.60 (2.87–6.75)
821	M	1,587	OU anisotropic	10.10 (8.26–12.12)	2.91 (2.38–3.49)
824	M	670	OU anisotropic	4.38 (3.53–5.32)	0.78 (0.63–0.95)
81C	F	188	OU anisotropic	2.16 (1.70–2.67)	0.49 (0.39–0.60)
823	F	39	OUf anisotropic	0.92 (0.63–1.25)	0.14 (0.10–0.20)

Code	Sex	Fixes	Selected model	AKDE 95% (95% CI)	AKDE 50% (95% CI)
822	F	190	OU anisotropic	0.51 (0.42–0.61)	0.07 (0.06–0.09)
814	M	24	OU anisotropic	0.09 (0.05–0.13)	0.02 (0.01–0.03)

AKDE home range estimates are given for the nine individuals that selected continuous-time range-residency movement models (Ornstein–Uhlenbeck family), ordered by decreasing AKDE 95%. Areas in hectares (95% CI); model selected by AICc. Individuals whose best model was IID (80C, 81E, 820, 825; AKDE ≡ KDE) and those with n < 5 fixes (80F, 81B) are not shown.

KDE 95% estimates were intermediate (median 2.2 ha) and MCP 95% the smallest (~2.0 ha). At 95%, MCP differed from KDE ($p = 0.022$) and from AKDE ($p = 0.012$), but KDE and AKDE did not differ ($p = 0.16$); at 50%, no comparison was significant (Table 8). This pattern reflects the tendency of MCP to underestimate the utilisation distribution, whereas AKDE incorporates trajectory autocorrelation.

Table 8. Statistical comparisons of *Mauremys rivulata* home ranges by sex and method.

Comparison	Test	N	p-value	Signif.
Sex (F vs M), MCP 95%	Mann–Whitney	11	0.181	n.s.
Sex (F vs M), KDE 95%	Mann–Whitney	11	0.456	n.s.
Sex (F vs M), AKDE 95%	Mann–Whitney	9	0.548	n.s.
Sex (F vs M), MCP 50%	Mann–Whitney	11	0.607	n.s.
Sex (F vs M), KDE 50%	Mann–Whitney	11	0.529	n.s.
Sex (F vs M), AKDE 50%	Mann–Whitney	9	0.548	n.s.
MCP 95% vs KDE 95%	Wilcoxon	15	0.022	*
KDE 95% vs AKDE 95%	Wilcoxon	9	0.164	n.s.
MCP 95% vs AKDE 95%	Wilcoxon	9	0.012	*
MCP 50% vs KDE 50%	Wilcoxon	15	0.229	n.s.
KDE 50% vs AKDE 50%	Wilcoxon	9	0.055	n.s.
MCP 50% vs AKDE 50%	Wilcoxon	9	0.203	n.s.

Sex effects by Mann–Whitney U (two-tailed); differences between estimators by individual-paired Wilcoxon test. n.s. = not significant; * $p < 0.05$.

Home-range size did not differ significantly between sexes for any estimator: AKDE 95% (Mann–Whitney $p = 0.55$), KDE 95% ($p = 0.46$), and MCP 95% ($p = 0.18$), with the same pattern at 50% (all $p > 0.5$; Table 8; Fig. 9A–B). Although the three largest areas belong to females, the low number of resident males limits test power, and this pattern was not interpreted as a sex effect. There was also no association between home-range size and number of fixes (Fig. 9C; Pearson: MCP 95% $R = 0.19$; KDE 95% $R = -0.10$; AKDE 95% $R = -0.13$). Thus, the largest areas mainly reflect the geometry of the occupied water body and the proximity of other elements of the water network to the occupied/resident water body, and not sex or tracking effort (Figure 9C).

A formal test of population or locality effects on home-range size was not possible, because eight of the nine range-resident individuals belong to the Konavle population and only one (823) to Zabrežje; the available contrast is therefore between habitat types within Konavle. Within that contrast, the descriptive pattern is consistent: individuals with nearby access to other water bodies and more structurally diverse habitat occupied larger ranges. Animals with access to longitudinal water bodies had the largest home ranges, whereas single-pond residents were the most confined. The per-individual 95% and 50% kernel-density areas are shown in Fig. 11.

AKDE 95% areas spanned more than three orders of magnitude among the nine residents (0.09–103.1 ha; median 4.4 ha, equivalent to a circle about 237 m in diameter). The largest areas were those of females 819 (103.1 ha, uphill forest pond, and downhill canal network, equivalent to a circle about 1,145 m in diameter), 816 (33.4 ha, canal), and 81F (22.0 ha, intermittent river Konavočica). Female 819, with the largest home range, occupies a linear complex with two cores: one along Konavle pond 1 (in spring 2025 and spring 2026), and another, linked via canal near pond 1 to downstream canals during the summer, autumn and winter months. By contrast, male 814 and female 822, restricted to a single pond in lowland Konavle, distant from other ponds and the fluvial network, showed the smallest home ranges, with 50% cores below 0.1 ha (0.09 ha and 0.51 ha, equivalent to circles only about 34 m and 81 m in diameter, respectively).

The data also indicate a clear effect of water-body geometry: the individuals that ranged most widely were those using longitudinal water bodies where movement is channelled along a one-dimensional corridor. The intermittent Konavočica River (core home range of female 81F) and the amelioration canals (core home range of female 816) were both used either over longer periods, or for short transits to the pond only. Pond residents with no fluvial network or nearby other ponds were spatially the most confined (814, 822, 820, 80f). When several ponds are available and sufficiently close, individuals included them in their core home range (e.g. female 823 in the two Majkovi ponds).

Pairwise spatial overlap

Pairwise spatial overlap, measured by the Bhattacharyya coefficient (BC), was low across the 55 dyads of the 11 adequately sampled individuals (Table 9; Figure 3C). Mean BC was 0.030 for female–female pairs (n = 28), 0.049 for female–male pairs (n = 24), and 0.000 for male–male pairs (n = 3). The contrast between male–male and female–female dyads was not significant in the individual-level permutation test (p = 0.67). The few values above zero occurred between individuals that shared the same water body, such as the Konavočica River stretch at Gruda settlement. Thus, using per-individual bandwidths, spatial overlap was low and showed no structuring by sex.

Table 9. Pairwise spatial overlap of *Mauremys rivulata* home ranges by dyad type.

Dyad	Pairs	Mean BC	Median BC	SD	Min.	Max.
F–F	28	0.030	0.000	0.122	0.000	0.613
F–M	24	0.049	0.000	0.169	0.000	0.732
M–M	3	0.000	0.000	0.000	0.000	0.000

Overlap for n = 11 adequately sampled individuals, 55 dyads. The Bhattacharyya coefficient (BC) ranges from 0 (no overlap) to 1 (identical distributions). Permutation test on the M–M vs. F–F mean difference: p = 0.67 (n.s.).

Habitat selection: integrated step-selection function (iSSF)

The integrated step-selection function, based on 2,506 used steps from eight individuals and 50 available steps for each used step (Table 5; Fig. 10), indicated strong selection for proximity to surface water. The coefficient of log distance to the hydrographic network was negative ($\beta = -0.359$ per SD, SE = 0.018, $p < 0.001$), with a relative selection strength of 0.70 per standard deviation. Thus, for each one-SD increase in log distance to water, the relative probability of selecting a step was multiplied by 0.70, showing that the turtles consistently selected steps close to water. Among the movement covariates, the turn-angle cosine was also strongly negative ($\beta = -0.839$ per SD, $p < 0.001$; RSS = 0.43), indicating tortuous and reversing movement rather than persistent directional displacement. Log step length had no significant effect ($\beta = -0.027$ per SD, $p = 0.19$; RSS = 0.97).

Table 5. Coefficients of the integrated step-selection function (iSSF).

Covariate (per SD)	β	SE	RSS = exp(β)	95% CI (RSS)	p
Log distance to water	−0.359	0.018	0.698	0.675–0.723	< 0.001
Turn-angle cosine	−0.839	0.020	0.432	0.415–0.450	< 0.001
Log step length	−0.027	0.021	0.973	0.935–1.013	0.189

iSSF coefficients are fitted by conditional logistic regression on 2,506 used steps (eight individuals), each matched to 50 available steps (one stratum per step). Covariates are z-standardised. RSS = exp(β) is the relative selection strength per standard deviation.

DISCUSSION

With respect to the STRANGE framework (Webster and Rutz 2020), we consider the sample inherently constrained by trap vulnerability biases. To mitigate personality-dependent capture bias, we carried out intensive trapping to obtain a pool of concurrent candidates at each location, randomising final tracker deployment among qualified adults, with individual differences visible in the results. However, a significant sampling asymmetry occurred between sexes. Therefore, sex-related questions are reported with sex treated

as an exploratory rather than confirmatory factor. Furthermore, instrumentation was restricted to individuals of adequate body condition to ensure ethical welfare, which skews our sample towards the healthier segment of the adult population. Animals were equipped with loggers designed to remain below the standard ≤ 5% body mass threshold of the smallest instrumented adult to minimise behavioural distortion. To minimise acclimation and habituation bias, we applied a lower threshold (≤ 2.5% body mass) with turtles monitored on site for a minimal period to observe natural post-attachment behaviour and released on site to prevent artificial habituation to laboratory and handling conditions. To account for life-history fluctuations and minimise bias in natural changes in responsiveness, active tracking covered different seasons (April 2025 to June 2026) and was explicitly partitioned into four distinct functional periods, effectively capturing seasonal variance in behavioural states and thermal niches. Social background, rearing history, genetic make-up, and experience are not expected to produce a biased sample since all tracked individuals were wild-caught, sexually mature adults from naturally occurring populations within the same hydrographic network (Adriatic basin). Localised genetic microstructures indicate animals belong to the same gene pool, with minor differences based on the isolation of the two sampled subpopulations (Varga et al. 2023). Pre-capture social hierarchies, and exact age/experience profiles are unknown, which is standard for wild semi-aquatic reptile telemetry. Inference is generalised strictly to wild, healthy adult cohorts of *M. rivulata* within Mediterranean hydrographic systems, with conservation implications focused on Croatia.

The hidden Markov model (HMM) indicated a clear two-state behavioural structure, Slow and Fast, both with high diagonal persistence ($P(S \rightarrow S) = 0.86$; $P(F \rightarrow F) = 0.89$). This result places *M. rivulata* among the freshwater turtles with the highest behavioural persistence (Bury 1979; Plummer and Shirer 1975; Lebboroni and Chelazzi 1991). We retained the reproducible, biologically interpretable two-state model (Pohle et al. 2017), which was stable across the metrics used in the subsequent analyses. In contrast, the optimum for the three-state model was poorly reproducible across initialisations (13/60), indicating a multimodal, poorly identified likelihood surface, a typical symptom of state over-fitting in real series.

513 Moreover, the positive within-individual autocorrelation in log step speed in the three-state model violates
514 the conditional independence assumed by the standard HMM, which, together with neglected higher-order
515 or semi-Markov state processes, is known to bias estimates and to favour models with more states than
516 actually exist (Pohle et al. 2017; Lawler et al. 2019). The high persistence of the Slow behavioural state
517 indicates stays lasting several hours in, or at the edge of, the resident water body similar to other freshwater
518 turtle species such as *E. orbicularis* (Morales et al. 2004; Langrock et al. 2012; Zucchini et al. 2016,
519 Marchand et al, 2021). The high persistence of the Fast behavioural state indicates multi-hour performance
520 blocks of tortuous, reversing locomotion in area- restricted search, consistent with active benthic foraging,
521 as shown by the strongly negative turn-angle cosine obtained. Expected behaviour in alternating large
522 temporal blocks could be characterised by targeted, multi-hour movements driven by opportunistic
523 landscape-level foraging (e.g. active benthic foraging) or reproductive dispersal between core aquatic and
524 terrestrial home-range units, interspersed with prolonged, uninterrupted periods of low-activity
525 thermoregulation imposed by ectothermic metabolic constraints. Further research is required to determine
526 whether these structured blocks of Slow and Fast activity reflect a strict diurnal activity pattern, as
527 documented for *E. orbicularis* (Marchand et al, 2021), or broader diel behavioural cycles.

528 Fast periods occurred at transmitter temperatures 4.7 °C higher than Slow periods ($p < 0.001$), as expected
529 in ectotherms, in which locomotor performance and directed movement depend on thermal activation and
530 are fully realised only above activity thresholds (Bennett 1980; Huey and Stevenson 1979; Hertz et al. 1993;
531 Angilletta 2009). It should be recalled that transmitter temperature is an integrated indicator of both
532 microhabitat and the animal's body, and not a direct measure of core body temperature.

533 The most relevant thermal pattern was seasonal: in August, during the heat peak, the lowest annual
534 proportion of the Fast state occurred (25.1%), consistent with the use of thermal refuges under maximum
535 ambient temperatures, as reported for other Mediterranean Geoemydidae (Gasith and Sidis 1985; Park et
536 al. 2025) or for other species' diel activity patterns (Marchand et al, 2021). This summer-peak retreat in
537 activity is a widely described pattern for terrestrial and semi-aquatic ectotherms that are forced to seek

thermal refuges when ambient temperatures approach the upper limits of tolerance: as air temperatures exceed critical thresholds, activity declines sharply because individuals retreat to cooler microhabitats, even while incurring substantial metabolic costs (Sinervo et al. 2010; Kearney 2013; Doucette et al. 2023). In turtles, this retreat may intensify into aestivation during periods of heat and drought, with reduced activity windows and energy budgets (Gibbons et al. 1983; Ligon and Peterson 2002), and deep or shaded water serving as the main available thermal refuge (Bury 1979). The loss of shaded areas, deep-water zones or rhithral water bodies during the hottest part of the year may therefore increase thermal stress and further shorten activity windows under Mediterranean warming.

These seasonal contrasts are best interpreted against the broader phenology of *M. rivulata*, for which annual life cycle dynamics and variability within the species areal remain poorly documented. We adopt deliberately cautious, functional terminology (putative mating, putative nesting, thermal peak, prebrumation, overwintering), because the underlying reproductive events were not observed directly in this study and the timing of activity differs markedly across the species' range. However, our observed April–May activity peak aligns with mating in the temperate northern range (the Balkans and northern Turkey), reported from April to June (Güçlü and Türkozan 2010; Mantziou and Rifai 2014), while in western Turkey animals are active from May to September and have been observed mating, foraging, and basking, with mating individuals also recorded in November (Güçlü and Türkozan 2010). By contrast, in the arid southern range, mating is reported to be more or less continuous from autumn to spring (November to April), peaking in January and February (Gasith and Sidis 1985; Mantziou and Rifai 2014).

Furthermore, the June–July peak in activity observed in this research is consistent with nesting, as reported in Štih Koren's thesis (2024), and with headstarting activities in the ongoing species conservation breeding programme in Croatia, where females captured from late May onwards carry calcified eggs and have been observed to oviposit in June and July. Previous research on the species in the Balkans and northern Turkey reports that eggs are laid from mid-May to July (Güçlü and Türkozan 2010; Mantziou and Rifai 2014). Dry-land fixes (30 m from the water body) by females may mark terrestrial nesting excursions starting in May.

563 The August activity retreat coincides with the reported thermal limits of the species, which does not usually
564 feed below about 13 °C or above about 30.5 °C and, at air temperatures above roughly 36 °C, floats just
565 below the water surface to avoid overheating (Sidis and Gasith 1985; Rifai and Amr 2004). It also parallels
566 the post-nesting abandonment of drying ponds and movement into insulated marshes described from radio-
567 tracking in northern Greece. We observed a similar overwintering period to that reported by Chelazzi et al.
568 (2007) in Greece, peaking from November to December with activity emerging from February to March.
569 Blocked GNSS fixes from late October until late February are consistent with brumation and overwintering
570 in or beside the occupied ponds/canals. NB-IoT transmission is blocked at depths exceeding 20–30 cm in
571 dry substrata, or at depths as shallow as 5–10 cm in water-saturated clay soils, sub-surface karst cavities,
572 rock fissures, or under thick dry-stone walls. Relatively high recorded temperature values in late February
573 and early March fixes (10.4 - 45.4 °C) reflect solar exposure of the carapace-mounted logger rather than
574 body temperature, and indicate emergence from brumation.

575 The external sensor temperature, found to be 0.7 °C higher in females, could be explained by
576 thermoregulatory behaviour, or by thermal inertia in females due to sexual dimorphism and their larger
577 size. This thermal effect requires additional research with a balanced ratio of male and female individuals.

578 Five of the seven traits were repeatable after FDR correction, with modest magnitudes ($R = 0.10–0.27$),
579 close to the lower bound of the typical ecological repeatability range for activity traits ($R \approx 0.2–0.4$; Réale
580 et al. 2007; Dammhahn et al. 2018) and below the general mean of behavioural repeatability reported in the
581 literature ($R \approx 0.37$; Bell et al. 2009; Nakagawa and Schielzeth 2010). This pattern qualitatively replicates
582 results described for other freshwater turtles tracked over long periods (Carter et al. 2013; Refsnider et al.
583 2015) and implies a high level of within-individual plasticity in the sample. This is consistent with the
584 growing recognition of consistent individual differences in long-lived turtles, such as Mediterranean
585 congeners or sympatric species, like the Spanish pond turtle (*Mauremys leprosa* (Schweigger)) and the
586 European pond turtle (*Emys orbicularis* (Linnaeus)), which show individual consistency in behavioural
587 responses across repeated trials (Ibáñez et al. 2018), and with long-lived turtles, such as the ornate box

588 turtle (*Terrapene ornata* (Agassiz)), which exhibits highly repeatable behavioural types within and across
589 years (Reed et al. 2023).

590 The use of autocorrelational kernel density estimation (AKDE) as the primary estimator was justified by
591 continuous-time movement-model selection: nine well-sampled individuals selected autocorrelated models
592 of the Ornstein–Uhlenbeck family, indicating range residency and supporting the use of this estimator
593 (Fleming et al. 2015; Calabrese et al. 2016; Silva et al. 2022). By explicitly incorporating the autocorrelation
594 of fixes, AKDE corrects the underestimation bias that affects conventional estimators when they are applied
595 to autocorrelated relocations, a well-documented problem in home-range estimator comparisons (Fleming
596 et al. 2015; Noonan et al. 2019). In the four individuals whose best model was IID, the absence of detectable
597 autocorrelation caused AKDE to coincide with KDE.

598 The statistical similarity between KDE and AKDE at 95% (Wilcoxon $p = 0.16$), together with the significant
599 underestimation by MCP ($p = 0.012$ vs. AKDE), shows that the convex hull of the points does not
600 adequately represent the extent of the utilisation distribution in autocorrelated trajectories. This is consistent
601 with the known sensitivity of MCP to extreme points and sampling intensity, and with its inability to
602 describe the intensity of space use (Burgman and Fox 2003). The resulting utilisation areas (median 95% =
603 3.1 ha) are markedly smaller than the 4 km-diameter buffers used for regional range mapping (Štih Koren
604 2024), underlining the strong site fidelity of the tracked animals.

605 The home-range size of individuals occupying longitudinal water bodies, or with two disconnected home-
606 range cores, aligns with the finding of Hou and Shi (2024) that, in freshwater turtles, the configuration and
607 linearity of the aquatic habitat (linear riverine systems versus confined ponds) often outweigh sex as a
608 determinant of home-range size, and that the same species can show very different areas among populations
609 depending on habitat structure. The importance of home ranges with multiple cores connected by proximity
610 to other elements of the water network and longitudinal geometry is consistent with the concluding remarks
611 of Levi et al. (2025) who explain that *M. rivulata* is highly reluctant to move on dry land, and is affected

612 by hydro-biological barriers as it relies on homing movements through either canals or open water in the
613 highly fragmented waterbodies of the Hula Lake hydrological complex in Israel.

614 Pairwise overlap measured by BC was low across all dyad types, indicating a spatial organisation centred
615 on a few discrete pond complexes, with no space sharing between individuals from different complexes at
616 the resolution of the GNSS fixes during the active season. This pattern of strong site fidelity is consistent
617 with the marked homing ability already demonstrated for the species in experimental displacements (Levi
618 et al. 2025). Because sex cannot be evaluated as a factor influencing overlap dynamics in this study, further
619 work is required to determine whether the pattern observed in Maximilian's snake-necked turtle
620 (*Hydromedusa maximiliani* (Mikan)) is also relevant for *M. rivulata*. In *H. maximiliani*, home range size
621 was similar between sexes, but males exhibited significantly higher spatial overlap probabilities, reflecting
622 a mate-searching grid structure (Famelli et al. 2025). This longitudinal use has a direct conservation
623 implication, because streams and canals connect otherwise discrete pond complexes and may act as the
624 main dispersal and gene-flow corridors; their continuity (avoiding canalisation barriers, culverts, and dry-
625 season interruption) therefore deserves explicit protection alongside the ponds themselves.

626 The integrated step-selection function (iSSF; Avgar et al. 2016; Fortin et al. 2005) confirmed the strong
627 affinity of *M. rivulata* for proximity to water. Log distance to the hydrographic network showed a relative
628 selection strength of 0.70 per SD ($p < 0.001$), indicating that proximity to water was the main habitat signal
629 in the trajectories. Unlike *E. orbicularis*, which among emydid turtles is the species that can move furthest
630 from wetlands and survive for days or even weeks on dry land (Ficetola and Bernardi 2006, Kis et al. 2024),
631 *M. rivulata* in our study was never found to depart more than 30 to 50 m from the water body
632 (Supplementary Figure S2). This result is consistent with the reported species' obligate dependence on
633 aquatic environments (Vamberger et al. 2014) and with evidence from experimental displacement studies
634 on *M. rivulata* (Levi et al. 2025). It also reinforces, through an independent movement-based analysis, the
635 conclusion obtained from the home ranges and the low spatial overlap: water bodies organise space use. A
636 strongly negative turn-angle cosine coefficient is comparable to movement geometries observed in other

chelonians and ectotherms navigating fragmented or agricultural mosaics. It is consistent with intensive food searching within the boundaries of productive areas (Sutor et al. 2024), or in situations in which forward-directed, straight movement is structurally penalised by the discrete boundaries of the complex aquatic network (Levi et al. 2025).

Conservation implications

The results obtained provide practical recommendations for the conservation of Croatian range-edge *M. rivulata* populations at the extreme north-western limit of the species' distribution, which are vital for mitigating anthropogenic pressure and fulfilling Natura 2000 conservation objectives within this unique Mediterranean karst landscape:

(i) The low spatial overlap and the concentration of individuals in discrete pond complexes indicate strong site fidelity during the active season. Each perennial pond (artificial or semi-natural secondary ponds) and canal, as well as the intermittent river Konavočica, should therefore be treated as a near- independent spatial unit, where local anthropogenic or environmental impacts are unlikely to be offset by movements of individuals from neighbouring water bodies. Conservation management and long-term monitoring should therefore be organised at the scale of distinct localised habitat units.

(ii) The reduction in activity at the August thermal peak identifies the hottest part of the year as a phase of greater vulnerability, during which the activity window contracts and dependence on thermal refuges is maximal. We therefore recommend maintaining shaded vegetation along the margins of perennial ponds, protecting terrestrial nesting microhabitats with partial shade, and ensuring perennial aquatic microhabitat for thermoregulation. Buffering the temperatures of both refuges and nesting sites enables retention of optimal temperature-dependent sex determination (TSD) in which high incubation temperatures typically produce females in the genus *Mauremys* (Mrosovsky and Yntema 1980; Ewert et al. 2005). Global warming represents a concrete risk of sex-ratio skew (Neuwald and Valenzuela 2011; Sinervo et al. 2010), and the

high, female-producing temperatures tend to be physiologically more stressful for embryos (Lawson and Rollinson 2021). A spatially explicit assessment of the magnitude and direction of this climatic effect at the Croatian range edge is beyond the scope of the present telemetric baseline; species-specific ecological niche or species-distribution modelling (Kornilev et al. 2017) under future climate scenarios would provide more precise projections of habitat hydrology and thermal suitability, and is recommended as the appropriate next step in evaluating designated areas for species protection.

(iii) Strong selection for proximity to the hydrographic network in the step-selection analysis, together with the watercourses layer used to delimit the area of habitat, indicates that longitudinal water bodies—the intermittent Konavočica River, amelioration canals, and karst streams—function both as foraging and movement habitat and as connective corridors between pond complexes; their continuity, water quality, and riparian shading should be safeguarded alongside the ponds themselves.

(iv) Nesting and overwintering sites were not mapped directly, but the seasonal pattern indicates their existence and importance: the June–July nesting window suggests terrestrial oviposition microhabitats adjacent to the water bodies (up to 30 m away), and the contraction of activity from the thermal peak into pre-brumation implies putative overwintering refuges, plausibly in insulated marsh substrate and shaded or stone dry-wall pond and channel margins. Protecting the terrestrial matrix surrounding the water bodies - partially shaded, undisturbed ground suitable for nesting and overwintering refuges - is therefore as important for the persistence of this range-edge population as the protection of the aquatic habitat itself.

(v) The timing of disruptive habitat management activities, such as flood protection and water management, should take into account species' seasonal patterns as well as their microhabitat requirements. During brumation, from October to early March, locations and activities that pose a risk of direct mortality should be avoided.

CONCLUSION

The two *M. rivulata* populations in Konavle and Majkovi, southern Croatia, at the extreme north-west of the species' range, revealed coherent and mutually reinforcing behavioural and spatial patterns that converge on a single ecological reading: a species tightly coupled to proximity to intermittent, perennial and ephemeral lentic and lotic elements in complex fluvial network and strongly regulated by temperature throughout the active season. Trajectories were best described by a two-state behavioural structure, with high persistence in each state, clearly separating phases of low locomotor activity during Thermal peak (Aug), Prebrumation (Sep–Oct) and Overwintering (Nov–Mar), and high locomotor activity during Nesting (Jun–Jul) and Putative mating (Apr–May) periods. The low transition frequency of the behavioural structure, together with the reversing and tortuous movement pattern revealed by step-selection analysis, indicates individuals that forage and thermoregulate within confined water bodies, rather than animals that move directionally between them.

This confined way of life proved closely linked to temperature, where the higher-activity state was associated with higher transmitter temperatures, as expected for the thermal dependence of locomotion in ectotherms, whereas the difference between sexes, although statistically detectable, was too small to support an interpretation of differentiated thermal use. This coupling between behavioural state and temperature, rather than between sex and temperature, reinforces the conclusion that activity is governed above all by the immediate thermal context. Against this backdrop, several behavioural traits proved repeatable, albeit with modest magnitudes, now including a thermal component that emerged with the increased sample. Individual consistency in the use of thermal microhabitats, even if slight, suggests that differences among individuals may have ecological relevance in a long-lived organism, although the small sample argues for caution and for the acquisition of activity measures independent of step speed before any inference about behavioural syndromes.

Spatially, home ranges varied widely among individuals and were not structured by sex. Home-range magnitude mainly tracked the proximity of other hydrological elements to the occupied core habitat, the

perennial water body. Secondary ponds, agricultural ponds in forest and in open agricultural mosaic, intermittent river channel, streams and canals were used as the core habitat. Several cores were used by individuals when available. Individuals selected steps that kept them close to the hydrographic network (within the 30 m), indicating the importance of spring ephemeral water bodies for habitat connectivity. The low overlap among individuals, without structure by dyad type, points to spatial organisation centred on discrete water body complexes, with strong site fidelity during the active season. This spatial structure did not remain static throughout the year: behavioural-state proportions and transmitter temperature varied markedly across the active season, with an activity peak in the putative nesting period and a sharp contraction at the summer thermal peak. This retreat in the hottest part of the year is compatible with the use of thermal refuges and identifies that window as the phase of greatest vulnerability to the warming projected for the Mediterranean.

Taken together, these results support three key conservation messages. Site fidelity implies that each freshwater core range should be treated as a natural unit of spatial management, whose loss would be unlikely to be offset by recolonisation from neighbouring ponds or streams. Extreme dependence on proximity to water dictates the importance of lotic and lentic water elements shown to function both as core habitats and connectivity corridors determining the size of home range. The contraction of activity under extreme temperatures, together with the obligate dependence on extreme water proximity independently confirmed by habitat selection, indicates that maintaining thermal refuges, such as colder water, riparian shading, and protected terrestrial nesting microhabitats, is decisive for the persistence of this range-edge population under climate warming.

LIST OF ABBREVIATIONS

ABS	Animal Behavior Society
AICc	Akaike information criterion with correction for small sample sizes
AKDE	Autocorrelational kernel density estimation of home range
ASAB	Association for the Study of Animal Behaviour
BC	Bhattacharyya coefficient
BIC	Bayesian information criterion
CCL	Curved carapace length
CI	95% confidence intervals
DBSCAN	Density-based spatial clustering of applications with noise
EPSG	European Petroleum Survey Group standardized database of numeric codes used globally to uniquely identify coordinate reference systems, map projections, and geodetic datums
FDR	False discovery rate
GNSS	Global navigation satellite system
GPS	United States operating global positioning system
GSM	Global system for mobile communications
HMM	Hidden Markov model
ICC1	Intraclass correlation coefficient
ID	Individual identification code
IID	Independent and identically distributed movement model
ISO	International organization for standardization
iSSF	Integrated step selection function
KDE	Kernel density estimation of home range
MCP	Minimum convex polygons estimation of home range

MINGOR	Ministry of economy and sustainable development of Republic of Croatia
NB-IoT	Narrow band internet of things
OU	Ornstein-Uhlenbeck movement model
RSS	Relative selection strength: Z-standardised coefficients
SCL	Straight carapace length
SD	Standard deviation
SE	Standard error
SSF	Step selection function
STRANGE	STRANGE framework: S – Social background, T – Trappability and self-selection, R – Rearing history, A – Acclimation and habituation, N – Natural changes in responsiveness, G – Genetic make-up, E – Experience
TSD	Temperature-dependent sex determination
UTM	Universal transverse Mercator projection

740

741

742

743

744

745

746

747

748

749

750

751

DECLARATIONS

Ethics approval and consent to participate: The research plan was evaluated as being in compliance with the Croatian Animal Welfare Act (NN 102/17) and received a positive opinion from the Bioethical Committee for Animal Protection and Welfare of the University of Zagreb Faculty of Agriculture (Class: 114-01/25-03/02; Ref. No.: 251-71-29-02/19-25-2, 11 February 2025). Permits for capture, handling, and instrumentation procedures involving protected species were issued by the Croatian Ministry of Economy and Sustainable Development (Permits No. UP/I-352-04/25-08/147 and UP/I-352-04/23-08/148). Consent to participate: Not applicable.

Consent for publication: Not applicable.

Data availability: The dataset supporting the conclusions of this article is available in the ZENODO repository**,** https://doi.org/10.5281/zenodo.21891797.

Conflicts of interest: The authors report no competing interests to declare.

Funding: Data acquisition for his research was co-funded by the LIFE21-NAT-HR-LIFE for Mauremys project (GA: 101071737), granted by the LIFE Programme of the European Union, and co-funded by the Environmental Protection and Energy Efficiency Fund and the Government of the Republic of Croatia Office for Cooperation with NGOs.

Author contributions: ***KKŠ***: Investigation (supporting). ***AN***: Investigation (supporting). ***MR***: Conceptualisation (equal); methodology (equal); data curation (equal); formal analysis (lead); visualisation (lead); writing – original draft (lead); writing – review and editing (supporting); ***CBLS***: methodology (supporting); formal analysis (equal); visualization (supporting); writing – original draft (supporting). ***AŠK***: Conceptualisation (equal); investigation (lead); data curation (equal); methodology (supporting); writing – review and editing (supporting); funding acquisition (supporting). ***DŠ***: Conceptualisation (equal); data curation (equal); methodology (equal); writing – original draft (supporting); writing – review and editing (lead); funding acquisition (lead), supervision.

Acknowledgements: We thank the Association Hyla (Boris Lauš), the Zoological Garden in Zagreb, Hrvatske vode, the Croatian national water authority, and the Public Institution for Management of Protected Natural Areas of Dubrovnik-Neretva County for their support.

LITERATURE CITED

Angilletta MJ. Thermal Adaptation: A Theoretical and Empirical Synthesis. Oxford: Oxford University Press; 2009; doi:10.1093/acprof:oso/9780198570875.001.1.

ASAB Ethical Committee/ABS Animal Care Committee. Guidelines for the ethical treatment of nonhuman animals in behavioural research and teaching. Animal Behaviour. 2023;195:I-XI; doi:10.1016/j.anbehav.2022.09.006.

Avgar T, Potts JR, Lewis MA, Boyce MS. Integrated step selection analysis: bridging the gap between resource selection and animal movement. Methods Ecol Evol. 2016;7(5):619–30; doi:10.1111/2041-210X.12528.

Avgar T, Lele SR, Keim JL, Boyce MS. Relative selection strength: quantifying effect size in habitat- and step-selection inference. Ecol Evol. 2017;7(14):5322–30; doi:10.1002/ece3.3122.

Bell AM, Hankison SJ, Laskowski KL. The repeatability of behaviour: a meta-analysis. Animal Behaviour. 2009;77(4):771–83; doi:10.1016/j.anbehav.2008.12.022.

Benjamini Y, Hochberg Y. Controlling the false discovery rate: a practical and powerful approach to multiple testing. J R Stat Soc Series B Methodol. 1995;57(1):289–300; doi:10.1111/j.2517-6161.1995.tb02031.x.

Bennett AF. The thermal dependence of lizard behaviour. Animal Behaviour. 1980;28(3):752–62; doi:10.1016/S0003-3472(80)80135-7.

Börger L, Franconi N, De Michele G, Gantz A, Meschi F, Manica A, Lovari S, Coulson T. Effects of sampling regime on the mean and variance of home range size estimates. J Anim Ecol. 2006;75(6):1393–405; doi:10.1111/j.1365-2656.2006.01164.x.

Boyce MS, Vernier PR, Nielsen SE, Schmiegelow FKA. Evaluating resource selection functions. Ecol Modell. 2002;157(2–3):281–300; doi:10.1016/S0304-3800(02)00200-4.

820 Brown DD, Kays R, Wikelski M, Wilson R, Klimley AP. Observing the unwatchable through acceleration
821 logging of animal behavior. Anim Biotelemetry. 2013;1(1):20; doi:10.1186/2050-3385-1-20.
822 Burgman MA, Fox JC. Bias in species range estimates from minimum convex polygons: implications for
823 conservation and options for improved planning. Anim Conserv. 2003;6(1):19–28;
824 doi:10.1017/S1367943003003044.
825 Bury RB. Population ecology of freshwater turtles. In: Harless M, Morlock H, editors. Turtles: Perspectives
826 and Research. New York (NY): Wiley; 1979. p. 571–602.
827 Calabrese JM, Fleming CH, Gurarie E. ctmm: an R package for analyzing animal relocation data as a
828 continuous-time stochastic process. Methods Ecol Evol. 2016;7(9):1124–32; doi:10.1111/2041-
829 210X.12559.
830 Carter AJ, Feeney WE, Marshall HH, Cowlishaw G, Heinsohn R. Animal personality: what are behavioural
831 ecologists measuring? Biol Rev. 2013;88(2):465–75; doi:10.1111/brv.12007.
832 Chelazzi G, Naziridis T, Benvenuti S, Ugolini A, Crivelli AJ. Use of river-wetland habitats in a declining
833 population of the terrapin (Mauremys rivulata) along the Strymon River, northern Greece. J Zool.
834 2007;271(2):154–61; doi:10.1111/j.1469-7998.2006.00193.x.
835 Cordero-Rivera A, Ayres C. A management plan for the European pond turtle (Emys orbicularis)
836 populations of the Louro river basin (northwest Spain). Biologia. 2004;14:161–71.
837 https://www.researchgate.net/publication/288606591_A_management_plan_for_the_European_pond
838 _turtle_Emys_orbicularis_populations_of_the_Louro_river_basin_Northwest_Spain. Accessed 15 Jan
839 2026.
840 Crnobrnja-Isailović J, Polović L, Ljubisavljević K, Čađenović N, Čubrić T, Haxhiu I. Diversity and
841 conservation status of batrachofauna and herpetofauna in the Lake Skadar region. In: The
842 Skadar/Shkodra Lake Environment. Cham, Switzerland: Springer; 2018. p. 383–414; doi:10.1007/978-
843 3-319-99250-1.

844 Dammhahn M, Dingemanse NJ, Niemelä PT, Réale D. Pace-of-life syndromes: a framework for the
845 adaptive integration of behaviour, physiology and life history. Behav Ecol Sociobiol. 2018;72(3):62;
846 doi:10.1007/s00265-018-2473-y.

847 Doucette LI, Duncan RP, Osborne WS, Evans M, Georges A, Gruber B, Sarre SD. Climate warming drives
848 a temperate-zone lizard to its upper thermal limits, restricting activity, and increasing energetic costs.
849 Sci Rep. 2023;13:9603; doi:10.1038/s41598-023-35087-7.

850 Ewert MA, Lang JW, Nelson CE. Geographic variation in the pattern of temperature-dependent sex
851 determination in the American snapping turtle (Chelydra serpentina). J Zool. 2005;265(1):81–95;
852 doi:10.1017/S0952836904006120.

853 Famelli S, Gruber B, Georges A, Ortiz C, Souza FL, Beroluci J. Space use and home range size of the
854 freshwater turtle Hydromedusa maximiliani (Testudines: Chelidae) in southeastern Brazil. Herpetol
855 Conserv Biol. 2025;20(1):67–81.
856 https://www.researchgate.net/publication/391316685_Space_Use_and_Home_Range_Size_of_the_Fr
857 eshwater_Turtle_Hydromedusa_maximiliani_Testudines_Chelidae_in_Southeastern_Brazil.
858 Accessed 15 Feb 2026.

859 Fieberg J, Kochanny CO. Quantifying home-range overlap: the importance of the utilization distribution. J
860 Wildl Manage. 2005;69(4):1346–59; doi:10.2193/0022-541X(2005)69[1346:QHOTIO]2.0.CO;2.

861 Fleming CH, Calabrese JM. A new kernel density estimator for accurate home-range and species-range
862 area estimation. Methods Ecol Evol. 2017;8(5):571–9; doi:10.1111/2041-210X.12673.

863 Fleming CH, Fagan WF, Mueller T, Olson KA, Leimgruber P, Calabrese JM. Rigorous home range
864 estimation with movement data: a new autocorrelated kernel density estimator. Ecology.
865 2015;96(5):1182–8; doi:10.1890/14-2010.1.

866 Forester JD, Im HK, Rathouz PJ. Accounting for animal movement in estimation of resource selection
867 functions: sampling and data analysis. Ecology. 2009;90(12):3554–65; doi:10.1890/08-0874.1.

868 Fortin D, Beyer HL, Boyce MS, Smith DW, Duchesne T, Mao JS. Wolves influence elk movements:
869 behavior shapes a trophic cascade in Yellowstone National Park. Ecology. 2005;86(5):1320–30;
870 doi:10.1890/04-0953.

871 Gasith A, Sidis I. Sexual activity in the terrapin, Mauremys caspica rivulata, in Israel, in relation to the
872 testicular cycle and climatic factors. Journal of Herpetology. 1985;19(2):254–60;
873 doi:10.2307/1564179.

874 Gibbons JW, Greene JL, Congdon JD. Drought-related responses of aquatic turtle populations. Journal of
875 Herpetology. 1983;17(3):242–6; doi:10.2307/1563826.

876 Glennie R, Adam T, Leos-Barajas V, Michelot T, Photopoulou T, McClintock BT. Hidden Markov models:
877 pitfalls and opportunities in ecology. Methods Ecol Evol. 2023;14(1):43–56; doi:10.1111/2041-
878 210X.13801.

879 Güçlü Ö, Türkozan O. Population structure of Mauremys rivulata in western Turkey. Turkish Journal of
880 Zoology. 2010;34:385–91; doi:10.3906/zoo-0811-18.

881 Hertz PE, Huey RB, Stevenson RD. Evaluating temperature regulation by field-active ectotherms: the
882 fallacy of the inappropriate question. American Naturalist. 1993;142(5):796–818; doi:10.1086/285573.

883 Hollander M, Wolfe DA, Chicken E. Nonparametric statistical methods. 3rd ed. Hoboken (NJ): John Wiley
884 & Sons; 2014.

885 Hou X, Shi H. Movement and home range of Amur soft-shell turtle (Pelodiscus maackii) in the Ussuri
886 River, Heilongjiang Province, China. Animals. 2024;14(7):1088; doi:10.3390/ani14071088.

887 Huey RB, Stevenson RD. Integrating thermal physiology and ecology of ectotherms: a discussion of
888 approaches. American Zoologist. 1979;19(1):357–66; doi:10.1093/icb/19.1.357.

889 Ibáñez A, Martín J, Gazzola A, Pellitteri-Rosa D. Freshwater turtles reveal personality traits in their
890 antipredatory behaviour. Behavioural Processes. 2018;157:142–7; doi:10.1016/j.beproc.2018.08.011.

Iverson JB. Patterns of survivorship in turtles (order Testudines). Canadian Journal of Zoology. 1991;69(2):385–91; doi:10.1139/z91-060.

Kays R, Crofoot MC, Jetz W, Wikelski M. Terrestrial animal tracking as an eye on life and planet. Science. 2015;348(6240):aaa2478; doi:10.1126/science.aaa2478.

Kearney MR. Activity restriction and the mechanistic basis for extinctions under climate warming. Ecol Lett. 2013;16(12):1470–9; doi:10.1111/ele.12192.

Klappstein NJ, Thomas L, Michelot T. Flexible hidden Markov models for behaviour-dependent habitat selection. Mov Ecol. 2023;11(1):30; doi:10.1186/s40462-023-00392-3.

Kornilev Y, Popgeorgiev G, Naumov B, Stoyanov A, Tzankov N. Updated Distribution and Ecological Requirements of the Native Freshwater Turtles in Bulgaria. Acta Zool Bulg. 2017;Suppl 10:65-76. https://acta-zoologica-bulgarica.eu/downloads/acta-zoologica-bulgarica/2017/supplement-10-65-76.pdf. Accessed 19 Feb 2026.

Langrock R, King R, Matthiopoulos J, Thomas L, Fortin D, Morales JM. Flexible and practical modelling of animal telemetry data: hidden Markov models and extensions. Ecology. 2012;93(11):2336–42; doi:10.1890/11-2241.1.

Lawler E, Whoriskey K, Aeberhard WH, Field C, Mills Flemming J. The conditionally autoregressive hidden Markov model (CarHMM): inferring behavioural states from animal tracking data exhibiting conditional autocorrelation. J Agric Biol Environ Stat. 2019;24(4):651–68; doi:10.1007/s13253-019-00366-2.

Lawson L, Rollinson N. A simple model for the evolution of temperature-dependent sex determination explains the temperature sensitivity of embryonic mortality in imperilled reptiles. Conserv Physiol. 2021;9(1):coab020; doi:10.1093/conphys/coab020.

Lebboroni M, Chelazzi G. Activity patterns of Emys orbicularis L. in central Italy. Ethol Ecol Evol. 1991;3(3):257–68; doi:10.1080/08927014.1991.9525373.

915 Lele SR, Merrill EH, Keim J, Boyce MS. Selection, use, choice and occupancy: clarifying concepts in
916 resource selection studies. J Anim Ecol. 2013;82(6):1183–91; doi:10.1111/1365-2656.12141.
917 Levi A, Meir O, Vilk O, Nathan R, Toledo S, Kolodny O, Vortman Y. Homing through ecological barriers
918 in Balkan pond turtles. Biol Lett. 2025;21:20240442; doi:10.1098/rsbl.2024.0442.
919 Ligon DB, Peterson CC. Physiological and behavioral variation in estivation among mud turtles
920 (Kinosternon spp.). Physiol Biochem Zool. 2002;75(3):283–93; doi:10.1086/342000.
921 Manly BFJ. Randomization, bootstrap and Monte Carlo methods in biology. 3rd ed. Boca Raton (FL):
922 Chapman and Hall/CRC; 2007v; doi:10.1201/9781315273075.
923 Manly BFJ, McDonald LL, Thomas DL, McDonald TL, Erickson WP. Resource selection by animals:
924 Statistical design and analysis for field studies. 2nd ed. Dordrecht, Netherlands: Springer; 2002; doi:
925 10.1007/0-306-48151-0.
926 Mann HB, Whitney DR. On a test of whether one of two random variables is stochastically larger than the
927 other. Annals of Mathematical Statistics. 1947;18(1):50–60; doi:10.1214/aoms/1177730491.
928 Mantziou G, Rifai L. Mauremys rivulata (Valenciennes in Bory de Saint-Vincent 1833) – Western Caspian
929 Turtle, Balkan Terrapin. In: Rhodin AGJ, Pritchard PCH, van Dijk PP, Saumure RA, Buhlmann KA,
930 Iverson JB, Mittermeier RA, editors. Conservation Biology of Freshwater Turtles and Tortoises.
931 Chelonian Research Monographs No. 5; 2014. p. 080.1–080.9;
932 doi:10.3854/crm.5.080.rivulata.v1.2014.
933 Marchand T, Le Gal AS, Georges JY. Fine scale behaviour and time-budget in the cryptic ectotherm
934 European pond turtle Emys orbicularis. PLOS ONE. 2021;16(10); doi:10.1371/journal.pone.0256549.
935 MINGOR. Management Plan for the Balkan Terrapin (Mauremys rivulata) with an Action Plan (in
936 Croatian). Ministry of Economy and Sustainable Development, Croatia; 2021.
937 https://mingo.gov.hr/UserDocsImages/UPRAVA%20ZA%20ZA%C5%A0TITU%20PRIRODE/Plan
938 _upravljanja_rije%C4%8Dnom_kornja%C4%8Dom_s_akcijskim_planom.pdf. Accessed 15 Mar
939 2026.

McClintock BT, Michelot T. momentuHMM: R package for generalized hidden Markov models of animal movement. Methods Ecol Evol. 2018;9(6):1518–30; doi:10.1111/2041-210X.12995.

McClintock BT, King R, Thomas L, Matthiopoulos J, McConnell BJ, Morales JM. A general discrete-time modeling framework for animal movement using multistate random walks. Ecol Monogr. 2012;82(3):335–49; doi:10.1890/11-0326.1.

McClintock BT, Langrock R, Gimenez O, Cam E, Borchers DL, Glennie R, Patterson TA. Uncovering ecological state dynamics with hidden Markov models. Ecol Lett. 2020;23(12):1878–1903; doi:10.1111/ele.13610.

Michelot T, Langrock R, Patterson TA. moveHMM: an R package for the statistical modelling of animal movement data using hidden Markov models. Methods Ecol Evol. 2016;7(11):1308–15; doi:10.1111/2041-210X.12578.

Michelot T, Storey E. Scale dependence in hidden Markov models for animal movement. arXiv preprint arXiv:2510.03958. 2025; doi:10.48550/arXiv.2510.03958.

Morales JM, Haydon DT, Frair J, Holsinger KE, Fryxell JM. Extracting more out of relocation data: building movement models as mixtures of random walks. Ecology. 2004;85(9):2436–45; doi:10.1890/03-0269.

Mrosovsky N, Yntema CL. Temperature dependence of sexual differentiation in sea turtles: implications for conservation practices. Biol Conserv. 1980;18(4):271–80; doi:10.1016/0006-3207(80)90003-8.

Nakagawa S, Schielzeth H. Repeatability for Gaussian and non-Gaussian data: a practical guide for biologists. Biol Rev. 2010;85(4):935–56; doi:10.1111/j.1469-185X.2010.00141.x.

Nathan R, Getz WM, Revilla E, Holyoak M, Kadmon R, Saltz D, Smouse PE. A movement ecology paradigm for unifying organismal movement research. Proc Natl Acad Sci U S A. 2008;105(49):19052–9; doi:10.1073/pnas.0800375105.

963 Neuwald JL, Valenzuela N. The lesser known challenge of climate change: thermal variance and sex-
964 reversal in vertebrates with temperature-dependent sex determination. PLOS ONE. 2011;6(3):e18117;
965 doi:10.1371/journal.pone.0018117.

966 Noonan MJ, Tucker MA, Fleming CH, Akre TS, Alberts SC, Ali AH, et al. A comprehensive analysis of
967 autocorrelation and bias in home range estimation. Ecol Monogr. 2019;89(2):e01344;
968 doi:10.1002/ecm.1344.

969 Park CD, Kwon K, Yoo J, Yoo N, Choi CY, Yoon JD. Spatial ecology and habitat use of the reeves' turtle
970 (Mauremys reevesii) in lentic and lotic systems. Anim Biotelemetry. 2026; doi:10.1186/s40317-026-
971 00481-1.

972 Patterson TA, Thomas L, Wilcox C, Ovaskainen O, Matthiopoulos J. State–space models of individual
973 animal movement. Trends Ecol Evol. 2008;23(2):87–94; doi:10.1016/j.tree.2007.10.009.

974 Patterson TA, Basson M, Bravington MV, Gunn JS. Classifying movement behaviour in relation to
975 environmental conditions using hidden Markov models. J Anim Ecol. 2009;78(6):1113–23;
976 doi:10.1111/j.1365-2656.2009.01583.x.

977 Patterson TA, Parton A, Langrock R, Blackwell PG, Thomas L, King R. Statistical modelling of individual
978 animal movement: an overview of key methods and a discussion of practical challenges. AStA Adv
979 Stat Anal. 2017;101(4):399–438; doi:10.1007/s10182-017-0302-7.

980 Plummer MV, Shirer HW. Movement patterns in a river population of the softshell turtle Trionyx muticus.
981 Occas Pap Mus Nat Hist Univ Kansas. 1975;43:1–26. https://archive.org/download/biostor-
982 50153/biostor-50153.pdf. Accessed 15 Feb 2026.

983 Pohle J, Langrock R, van Beest FM, Schmidt NM. Selecting the number of states in hidden Markov models:
984 pragmatic solutions illustrated using animal movement. J Agric Biol Environ Stat. 2017;22(3):270–93;
985 doi:10.1007/s13253-017-0283-8.

Popgeorgiev G. Spatial distribution of Emys orbicularis (L., 1758) and Mauremys rivulata (Valenciennes, 1833) in the lower Veleka River, Bulgaria. Acta Zool Bulg. 2017;Suppl 10:129-132. http://www.faunacarpatica.sk/dokumenty/proceedings_2017.pdf

R Core Team. *R: A language and environment for statistical computing*. Vienna, Austria: R Foundation for Statistical Computing; 2026.

Réale D, Reader SM, Sol D, McDougall PT, Dingemanse NJ. Integrating animal temperament within ecology and evolution. Biol Rev. 2007;82(2):291–318; doi:10.1111/j.1469-185X.2007.00010.x.

Reed BM, Hobelman K, Gauntt A, Schwenka M, Trautman A, Wagner P, et al. Spatiotemporal variation of behavior and repeatability in a long-lived turtle. Behav Ecol Sociobiol. 2023;77(7):88; doi:10.1007/s00265-023-03360-4.

Refsnider JM, Reedy AM, Warner DA, Janzen FJ. Do trade-offs between predation pressures on females versus nests drive nest-site choice in painted turtles? Biol J Linn Soc. 2015;116(4):847–55; doi: 10.1111/bij.12671.

Rifai L, Amr Z. Morphometrics, distribution and ecology of the freshwater turtles (Order Testudines) of Jordan. Denisia. 2004;14:317–33.

Rowe JW, Dalgarn SF. Home range size and daily movements of midland painted turtles (Chrysemys picta marginata) in relation to body size, sex, and weather patterns. Herpetol Conserv Biol. 2010;5(3):461–73; doi:10.1670/0022-1511(2003)037[0342:AAMOMP]2.0.CO;2.

Seaman DE, Millspaugh JJ, Kernohan BJ, Brundige GC, Raedeke KJ, Gitzen RA. Effects of sample size on kernel home range estimates. J Wildl Manage. 1999;63(2):739–47; doi:10.2307/3802664.

Seware BZ. Karst topography: Formation, processes, characteristics, landforms, degradation and restoration: A systematic review. Watershed Ecol Environ. 2024;6:252-69; doi:10.1016/j.wsee.2024.10.003.

Sidis I, Gasith A. Food habits of the Caspian terrapin (Mauremys caspica rivulata) in unpolluted and polluted habitats in Israel. J Herpetol. 1985;19(1):108–15; doi:10.2307/1564426.

1011 Signer J, Fieberg J, Avgar T. Animal movement tools (amt): R package for managing tracking data and
1012 conducting habitat selection analyses. Ecol Evol. 2019;9(2):880–90; doi:10.1002/ece3.4823.
1013 Sih A, Bell A, Johnson JC. Behavioral syndromes: an ecological and evolutionary overview. Trends Ecol
1014 Evol. 2004;19(7):372–8; doi:10.1016/j.tree.2004.04.009.
1015 Silva I, Fleming CH, Noonan MJ, Alston J, Folta C, Fagan WF, Calabrese JM. Autocorrelation-informed
1016 home range estimation: a review and practical guide. Methods Ecol Evol. 2022;13(3):534–44;
1017 doi:10.1111/2041-210X.13786.
1018 Silverman BW. Density estimation for statistics and data analysis. London, England: Chapman and Hall;
1019 1998; doi:10.1201/9781315140919.
1020 Sinervo B, Méndez-de-la-Cruz F, Miles DB, Heulin B, Bastiaans E, Villagrán-Santa Cruz M, et al. Erosion
1021 of lizard diversity by climate change and altered thermal niches. Science. 2010;328(5980):894–99;
1022 doi:894–899. 10.1126/science.1184695.
1023 Stoffel MA, Nakagawa S, Schielzeth H. rptR: repeatability estimation and variance decomposition by
1024 generalized linear mixed-effects models. Methods Ecol Evol. 2017;8(11):1639–44; doi:10.1111/2041-
1025 210X.12797.
1026 Sutor S, McIntyre NE, Griffis-Kyle KL. Vegetation cover, topography, and low-traffic roads influence
1027 Sonoran desert tortoise (Gopherus morafkai) movement and habitat selection. Mov Ecol. 2024;12:68;
1028 doi:10.1186/s40462-024-00503-8.
1029 Štih Koren A. Distribution, morphological and ecological characteristics of the Balkan terrapin, Mauremys
1030 rivulata (Valenciennes 1833) in Croatia [Doctoral dissertation]. Zagreb, Croatia: University of Zagreb
1031 Faculty of Science; 2024. https://repozitorij.pmf.unizg.hr/en/object/pmf:13908. Accessed 15 Feb 2026.
1032 Thomson SA. Turtles of the world: annotated checklist and atlas. Phyllomedusa. 2021;20(2):225–8;
1033 doi:10.11606/issn.2316-9079.v20i2p225-228.
1034 Thurfjell H, Ciuti S, Boyce MS. Applications of step-selection functions in ecology and conservation. Mov
1035 Ecol. 2014;2:4; doi:10.1186/2051-3933-2-4.

1036 Vamberger M, Stuckas H, Ayaz D, Lymberakis P, Široký P, Fritz U. Massive transoceanic gene flow in a
1037 freshwater turtle (Testudines: Geoemydidae: Mauremys rivulata). Zool Scr. 2014;43:313–22;
1038 doi:10.1111/zsc.12055.
1039 Varga F, Krstulović D, Galov A, Štih Koren A, Šalamon D. Genetic tools and approaches for conservation
1040 management of Mauremys rivulata in Croatia [Abstract]. In: Carović-Stanko K, Širić I, editors. 58th
1041 Croatian & 18th International Symposium on Agriculture: Book of abstracts. Zagreb, Croatia: Faculty
1042 of Agriculture, University of Zagreb; 2023. p. 92. https://www.croris.hr/crosbi/publikacija/prilog-
1043 skup/732757. Accessed 15 Feb 2026.
1044 Webster MM, Rutz C. How STRANGE are your study animals? Nature. 2020;582(7812):337-40;
1045 doi:10.1038/d41586-020-01751-5.
1046 Wilcoxon F. Individual comparisons by ranking methods. Biometrics Bulletin. 1945;1(6):80–3;
1047 doi:10.2307/3001968.
1048 Winner K, Noonan MJ, Fleming CH, Olson KA, Mueller T, Sheldon D, et al. Statistical inference for home-
1049 range overlap. Methods Ecol Evol. 2018;9(7):1679–1691; doi:10.1111/2041-210X.13027
1050 Worton BJ. Kernel methods for estimating the utilization distribution in home-range studies. Ecology.
1051 1989;70(1):164–8; doi:10.2307/1938423.
1052 Zucchini W, MacDonald IL, Langrock R. Hidden Markov Models for Time Series: An Introduction Using
1053 R. 2nd ed. Boca Raton (FL): Chapman and Hall/CRC; 2016; doi:10.1201/b20790.

1054

1055

1056

1057

1058

TABLES

FIGURES

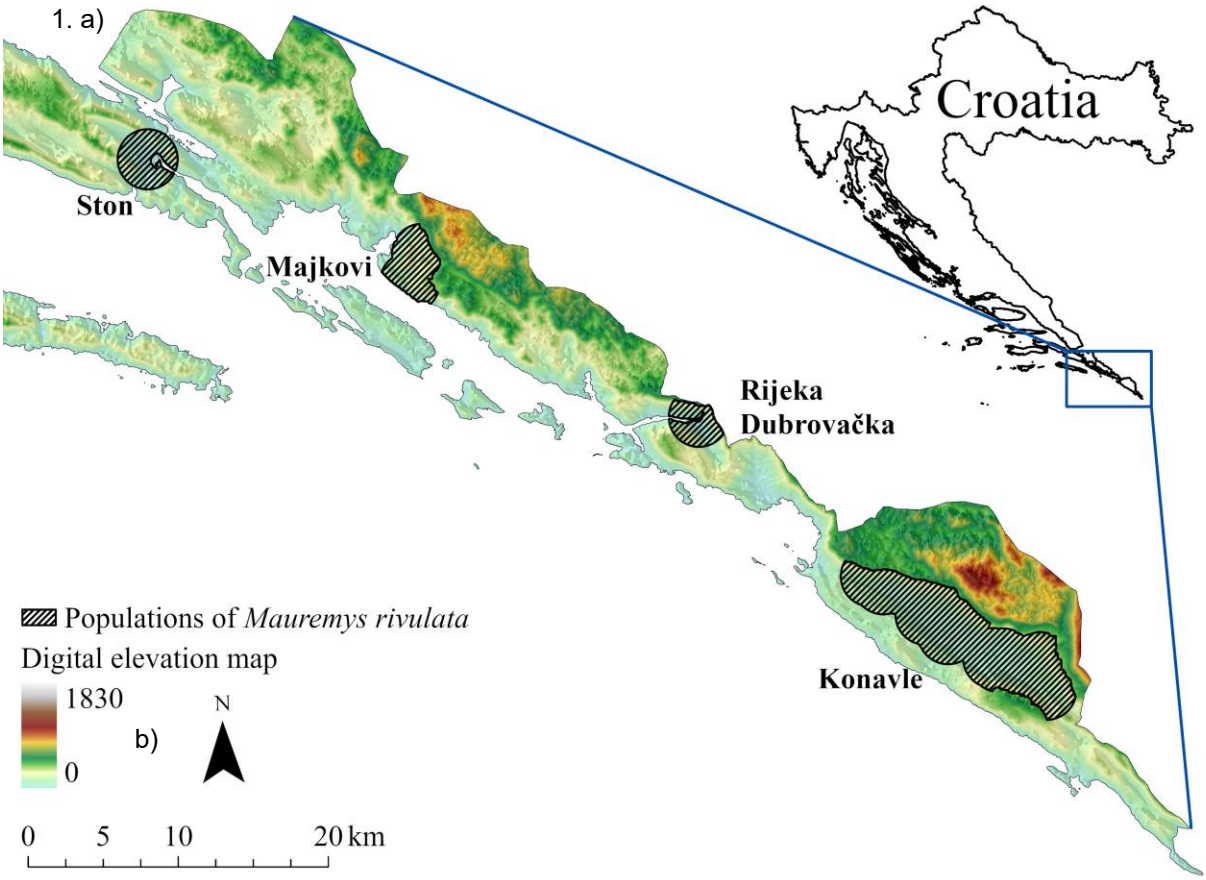


Figure 1. *Mauremys rivulata* populations in Croatia from north to south: Ston, Majkovi, Ombla, Konavle population (adapted from regional range mapping in Štih Koren, 2024), with trackers deployed in the viable Majkovi and Konavle populations.

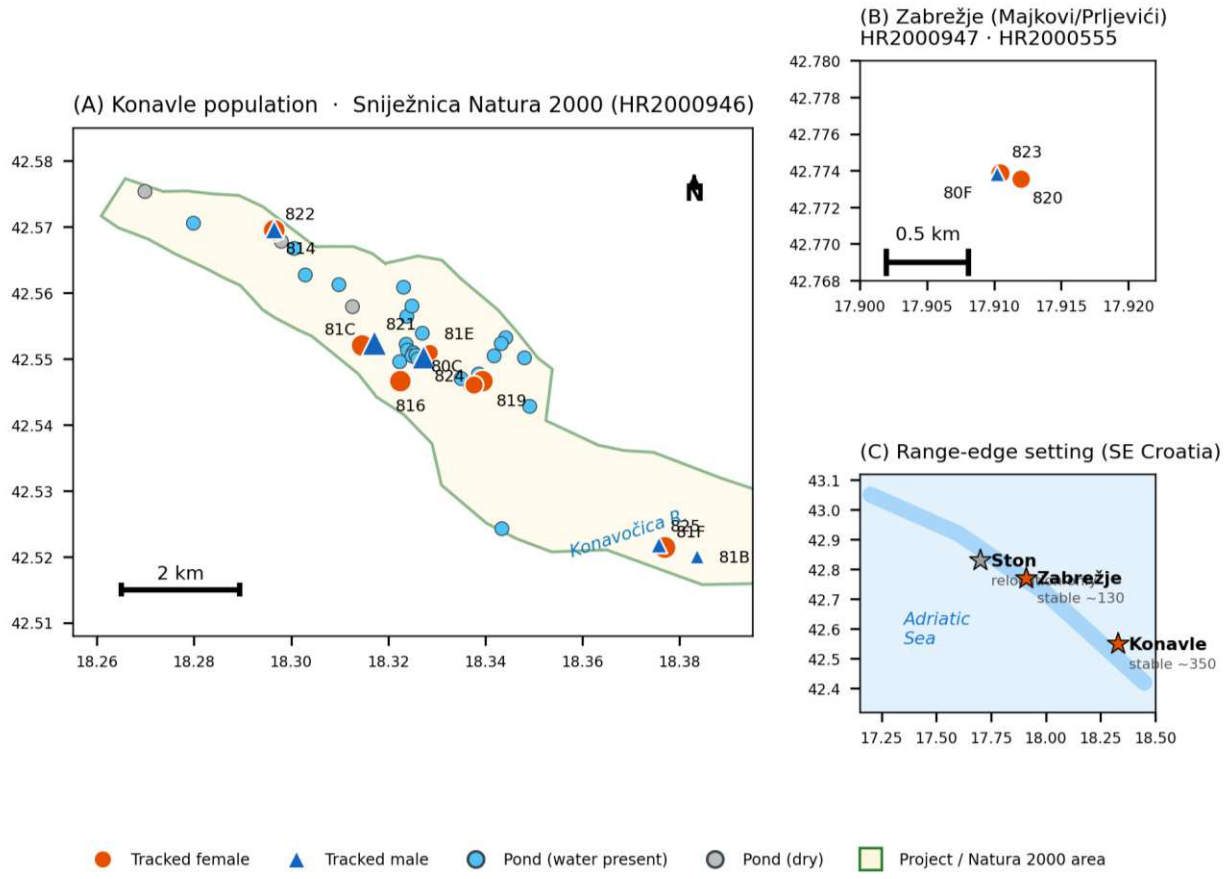


Figure 2. Behavioural states and thermal niche. (A) BIC by number of HMM states; the two-state model (circled) was retained despite a marginally lower BIC for k = 3 (see Results). (B) State emission distributions over log step speed. (C) Estimated transition probabilities.

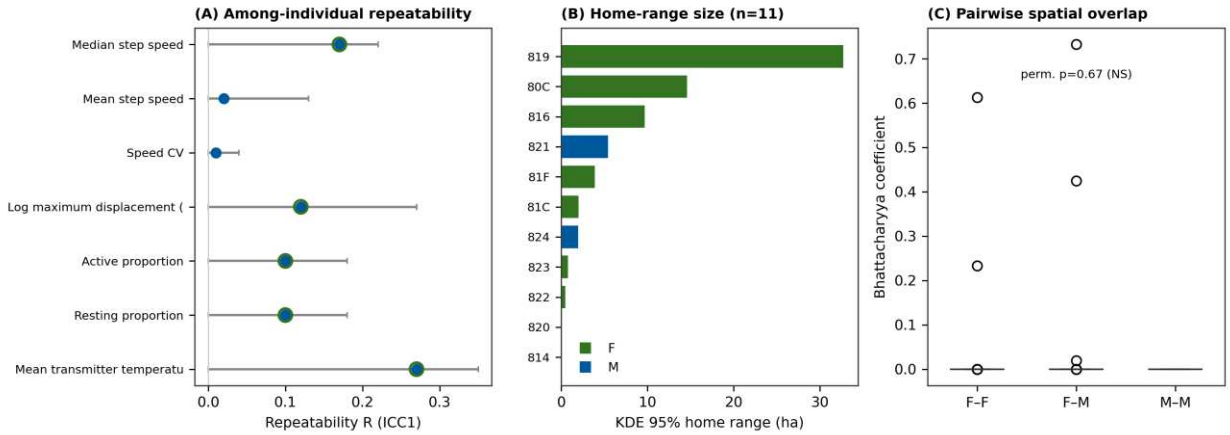


Figure 3. (A) Among-individual repeatability (ICC1) of seven behavioural traits with 95% CI by clustered bootstrap; traits significant after FDR correction are circled. (B) Home-range size (KDE 95%) for the 11 adequately sampled individuals, coloured by sex. (C) Pairwise Bhattacharyya overlap by dyad type. Labels in the original are in English.

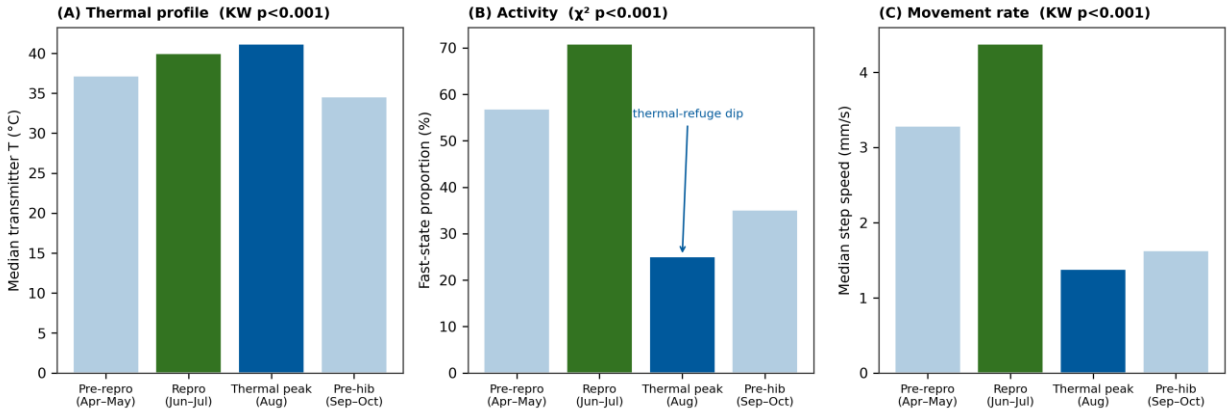
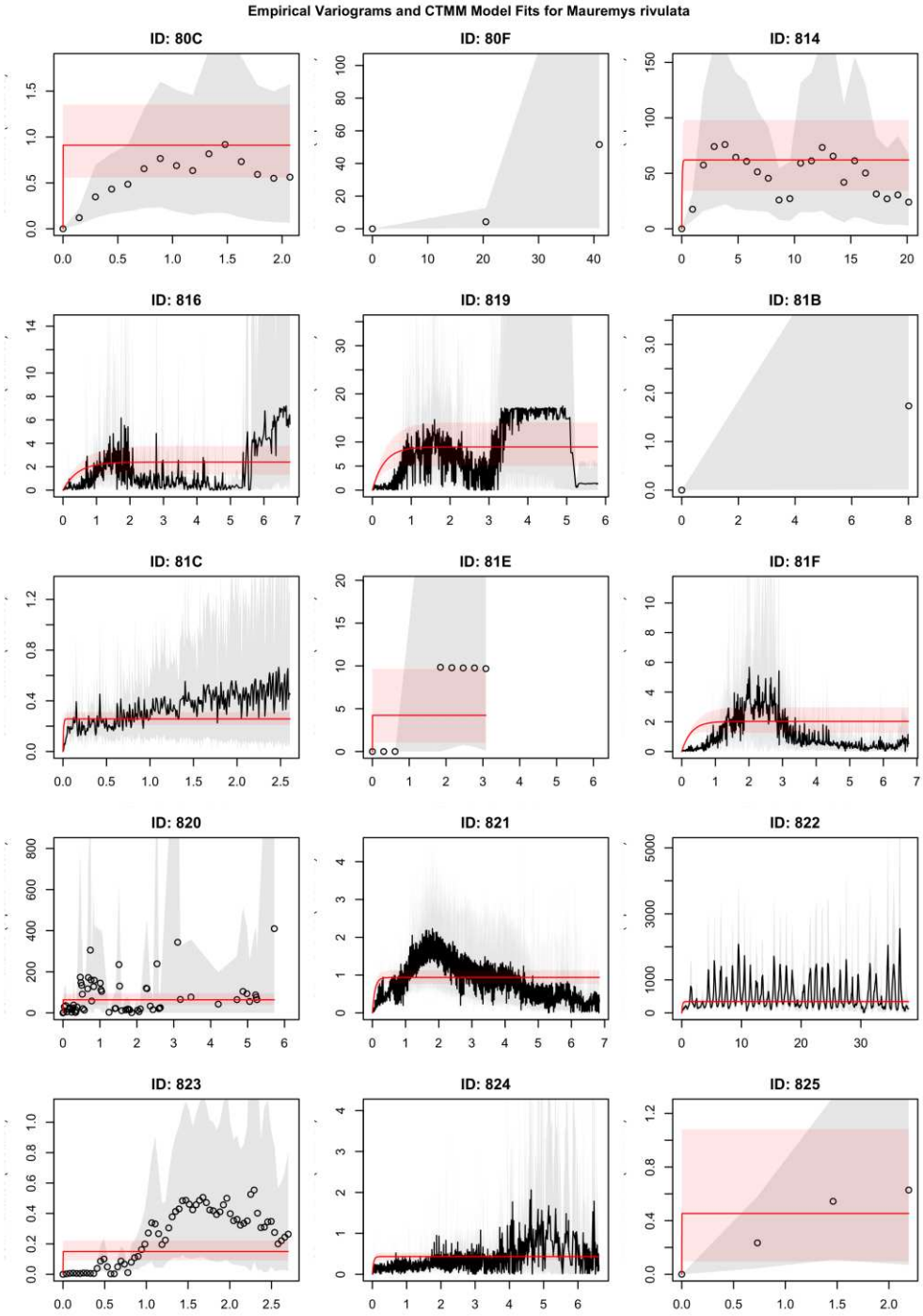


Figure 4. Seasonal variation across four functional periods of the active season. (A) Median transmitter temperature. (B) Fast-state proportion, showing the August thermal-refuge drop. (C) Median step speed. All among-period tests significant at $p < 0.001$.



1093

1094 **Figure 5.** Empirical variograms and continuous-time movement-model (ctmm) fits for the 15 individuals.

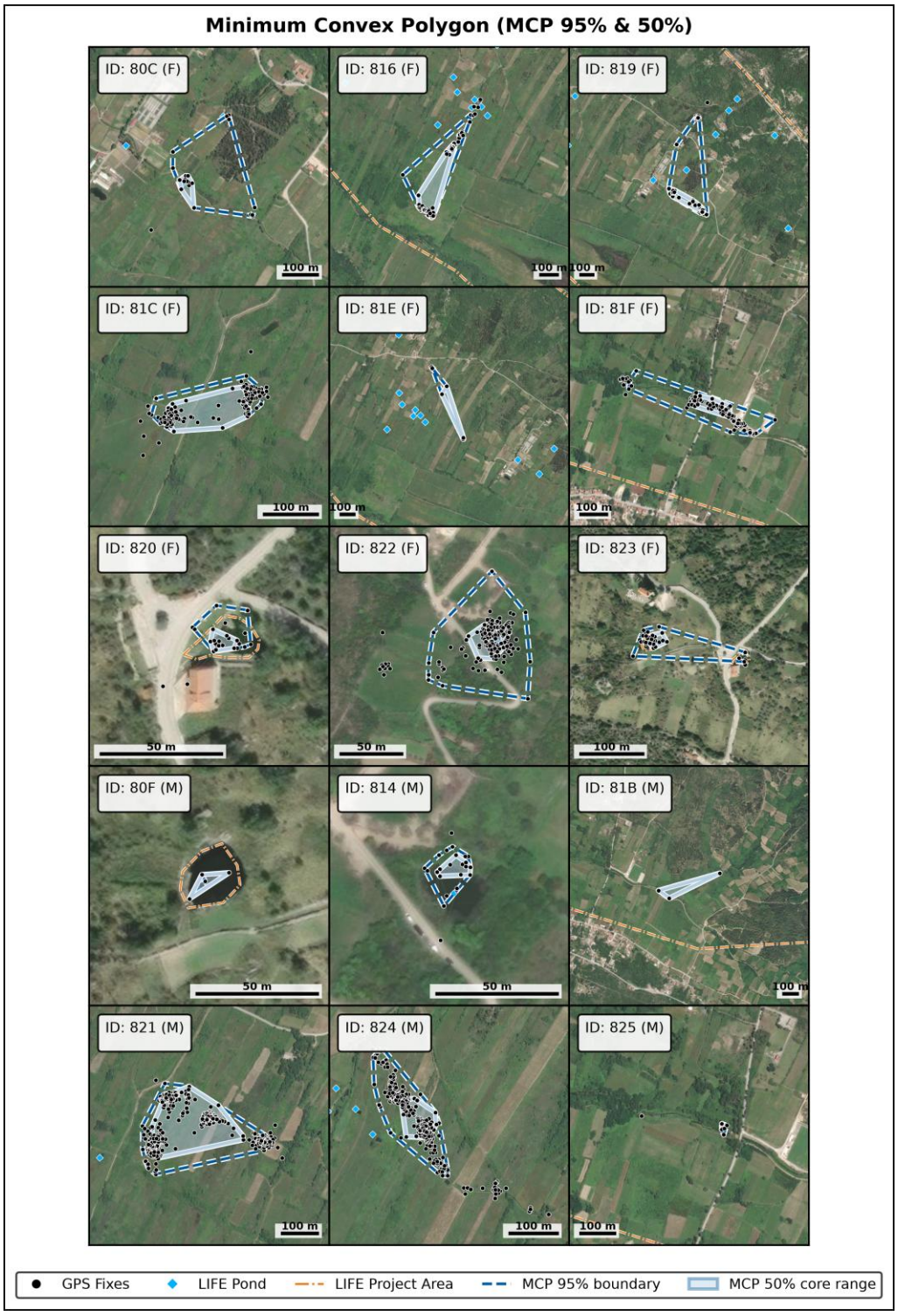


Figure 6. Minimum convex polygons (MCP 95% and 50% core) of the GNSS-active individuals over satellite imagery, with the GNSS fixes, the LIFE project ponds, and the project-area boundaries.



Figure 7. Kernel density estimates (KDE 95% and 50% core, per-individual Silverman bandwidth) of the GNSS-active individuals.



Figure 8. Autocorrelation-corrected kernel density (AKDE 95% and 50% core) for the nine individuals that selected range-residency models (Ornstein–Uhlenbeck family).

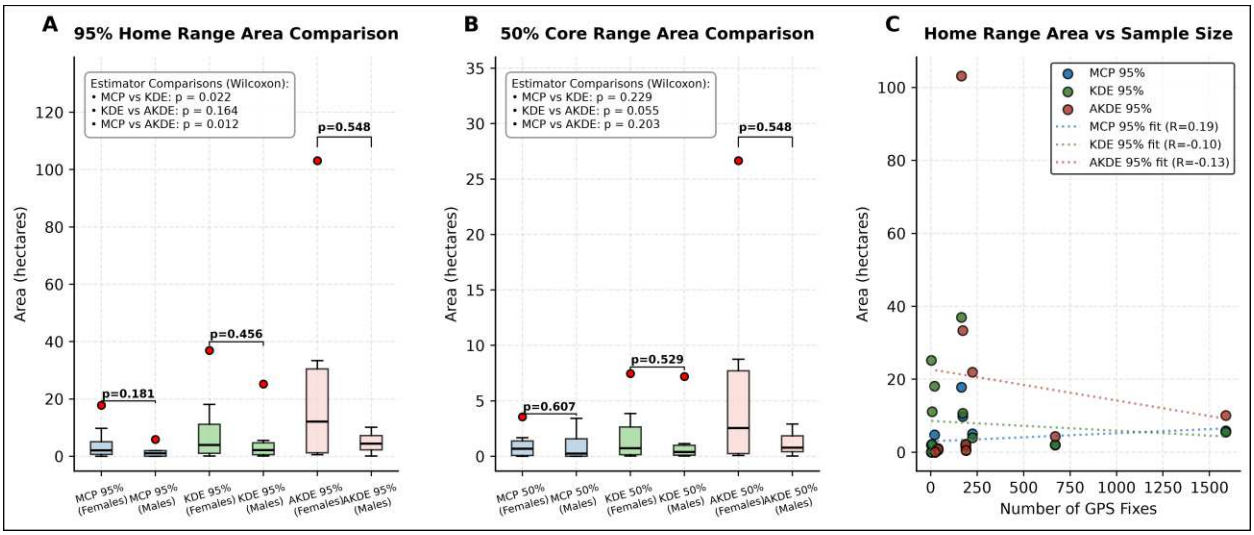


Figure 9. Statistical comparison of home-range estimators. (A) 95% home range by estimator (MCP, KDE, AKDE) and by sex, with Mann–Whitney p-values between sexes and Wilcoxon p-values between estimators. (B) 50% core, same conventions. (C) Home-range size as a function of the number of GNSS fixes, with trend lines and Pearson correlation coefficients per estimator (MCP 95% R = 0.19; KDE 95% R = −0.10; AKDE 95% R = −0.13).

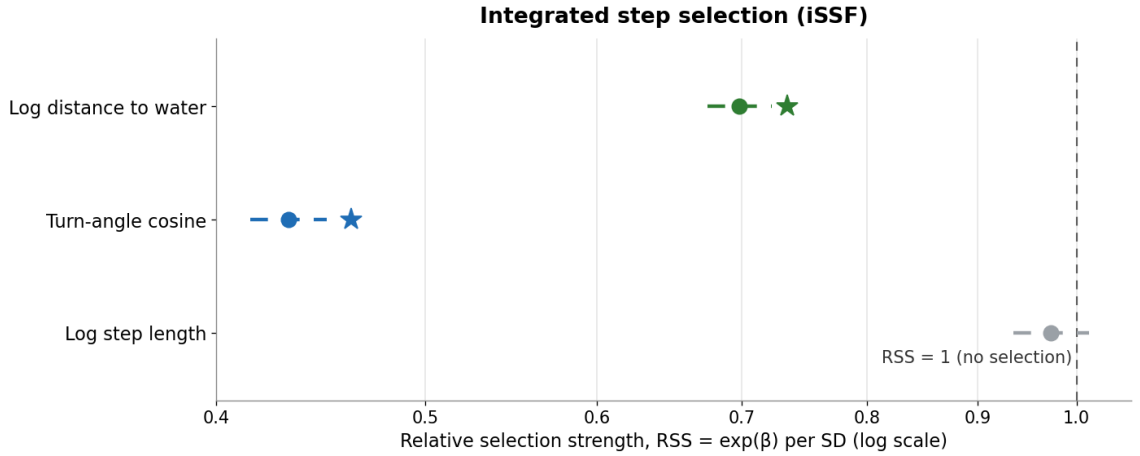


Figure 10. Coefficients of the integrated step-selection (iSSF) as relative selection strengths (RSS = exp(β)) per standard deviation.

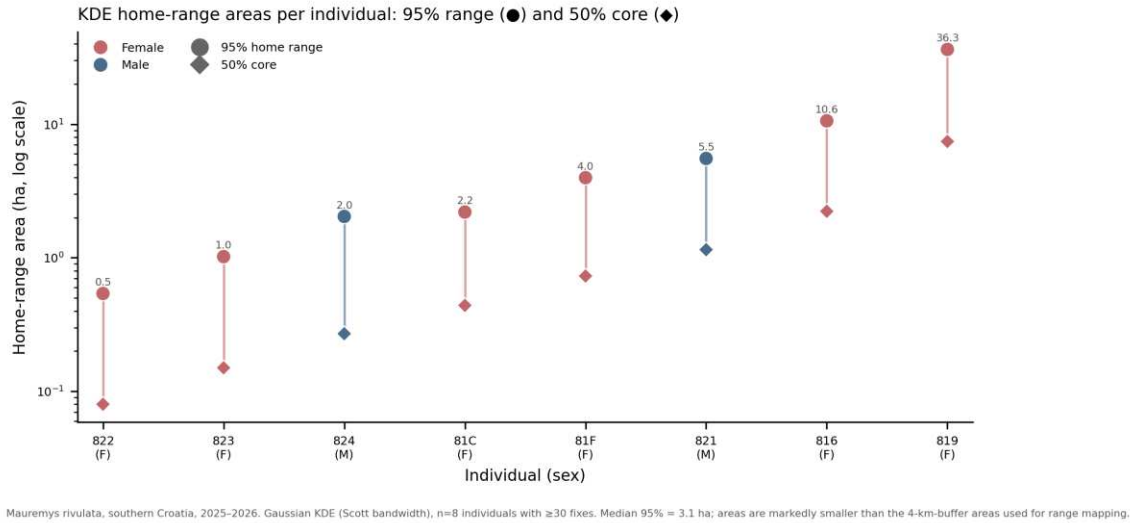


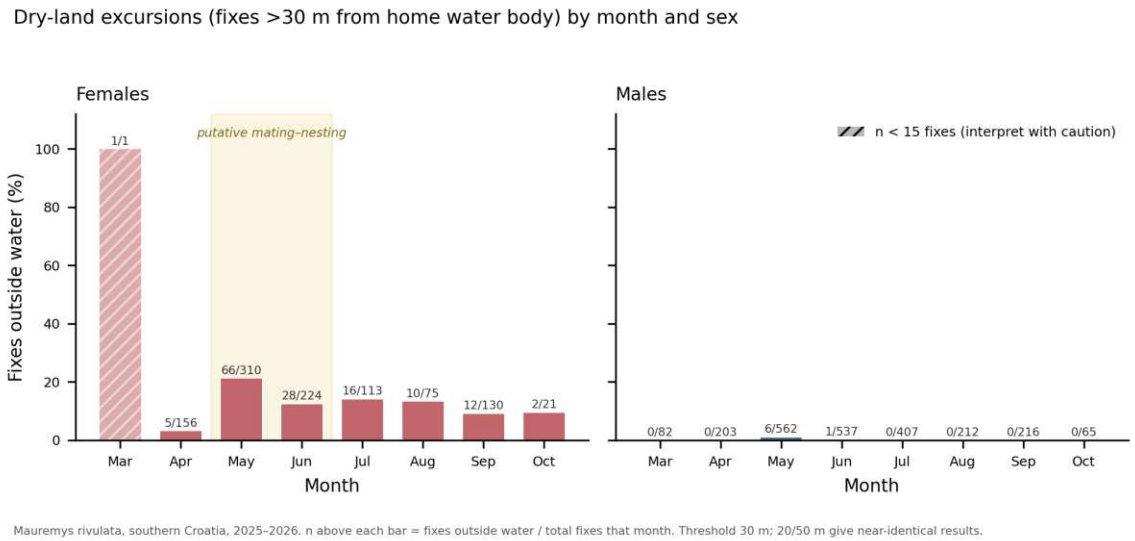
Figure 11. Individual home-range areas of *Mauremys rivulata* estimated by kernel density estimation (KDE; Gaussian kernel, Scott bandwidth), for the eight individuals with at least 30 GNSS fixes. Circles show the 95% home-range area and diamonds the 50% core area (hectares, log scale), coloured by sex and ordered by increasing 95% area; vertical stems link the core to the full range of each individual. The median 95% area was 3.1 ha (range 0.5–36.3 ha) and the median 50% core 0.58 ha. These utilisation-based areas are substantially smaller than the 4 km-diameter buffers used for regional range mapping (Fig. 1), reflecting the strong site fidelity of the tracked animals.

SUPPLEMENTARY MATERIAL

Supplementary Table S1. Body size and mass of the instrumented *Mauremys rivulata* adults, measured at capture (April 2025). SCL, straight carapace length; CCL, curved carapace length; Mass, body mass before release. Dashes indicate measurements not taken (e.g., device interference) or individuals not measured. Individuals 80C, 81E, 817 and 825 lack full biometrics. Sexes match the telemetry dataset.

Code	Sex	Locality	SCL (mm)	CCL (mm)	Mass (g)	Measured
80F	M	Majkovi (church)	122.9	123.7	676	—
823	F	Majkovi (church)	117.6	120.0	700	—
820	F	Majkovi (DVD)	104.2	105.5	676	—
821	M	Konavle (west)	154.3	—	363	25.4.2025.
81C	F	Konavle (west)	167.5	—	509	25.4.2025.
824	M	Konavle (east)	157.2	—	407	25.4.2025.
816	F	Konavle (east)	166.4	—	535	25.4.2025.
80C	F	Konavle (east)	—	—	—	25.4.2025.
819	F	Konavle (above road)	187.8	—	761	25.4.2025.
81F	F	Konavočica River	171.0	—	552	25.4.2025.
814	M	Konavle (upper)	—	—	459	25.4.2025.
822	F	Konavle (upper)	—	—	700	25.4.2025.
81B	M	Konavočica River (Gruda)	182.1	—	635	28.4.2025.
825	M	Konavočica River (Gruda)	—	—	—	—
817	M	Prljevići	—	—	—	—
81E	F	Konavle (east)	—	—	—	—

Summary: SCL 153.1 ± 28.5 mm (n = 10; females 152.4 ± 33.3, n = 6; males 154.1 ± 24.3, n = 4; Mann–Whitney p = 0.914). Mass 581 ± 129 g (n = 12; females 633 ± 99, n = 7; males 508 ± 140, n = 5; p = 0.087). Values are mean ± SD.



1143

1144 **Supplementary Figure S2.** Dry-land excursions of Mauremys rivulata by month and sex, southern Croatia,
1145 2025–2026. Bars show the percentage of GNSS fixes located outside water (more than 30 m from the
1146 individual's home water body) for females (left) and males (right). Numbers above each bar give the count
1147 of fixes outside water over the total fixes recorded that month. Hatched bars mark months with fewer than
1148 15 fixes, which should be interpreted with caution. The shaded band indicates the putative mating–nesting
1149 window (May–July). Females make dry-land movements throughout the active season, peaking during the
1150 putative nesting window, whereas males are almost exclusively aquatic apart from a small spring signal;
1151 classification is robust to the distance threshold (20, 30, and 50 m give near-identical results).